Coquimbo, August 07 of 2016

Dear Dr. John Huthnance
Editor, Ocean Science

In this document we are including a comment-by-comment response to the reviewers' comments regarding our manuscript "*Seasonal variability of the Ekman transport and pumping in the upwelling system off central-northern Chile (~30°S) based on a high-resolution atmospheric regional model (WRF)*". In addition, we provide a marked-up version of the manuscript showing the changes made using track-changes in Word to reply to the reviewers comments.

The main changes made to the manuscript were:

1. A paragraph that compares winds (from WRF) in the afternoon, evening and daily average for spring was added.

2. Materials and methods are improved

3. Chapter 3.3 was improved

4.- Summary was added

5.- The figures 2 and 8 were improved

We greatly appreciate the constructive and thoughtful comments of both reviewers, and we believe this revised version addresses them.

Best Regards,

Dr. Luis Bravo

RESPONSE TO REFEREE #1

We would like to begin our response by thanking the reviewer for his/her insightful comments we believe that our manuscript has been improved after addressing the recommended suggestions and comments

Specific comments:

1.- Influence of Diurnal Cycle There is a substantial change in the wind stress and wind stress curl diurnally. Does this impact the relative contribution from month to month?

First, we must clarify that the outputs of the WRF simulations are instantaneous wind values every hour, which later become daily averages. We know that by estimating daily averages it smoothens the influence of the wind's diurnal cycle, which is important considering the intensification of the coastal jet during the afternoon, but this does not mean the disappearance of the low frequency signal (subinertial variability), which is what we are interested in this work (see Figure 1).

In our study region, the atmospheric coastal jet extends from the coast for several tens of kilometers to the west, showing some nearshore maximums, like in Punta Lengua de Vaca (Garreaud and Muñoz, 2005; Muñoz and Garreaud, 2005, among others). In addition, near Punta Lengua de Vaca it has been found an atmospheric local and baroclinic jet (local origin), with a marked diurnal cycle, with a maximum around 18:00 (LT) (Garraeud et al, 2011; Rahn et al, 2011). Which confirms what the reviewer said.

On the other hand, we understand the meaning of the comment made by the reviewer. Therefore, differences in monthly estimates are analyzed using the proposed two-hour from the daily cycle instead of using daily averages (see replies below).

Overall, considering the objectives and the results shown in Figure 1, the daily cycle and specifically the intensification of the wind stress in the afternoon did not significantly affect the results.

However, given the importance of the daily cycle in the area and its intensification in the afternoon, we included a paragraph in the discussion regarding this issue and what would happen if only the afternoon information is included.

2.- It was never clearly stated, but what is the “daily output” (3014, line 26)?

We consider that the use of daily output is not appropriate therefore we changed it to daily averages obtained from hourly simulations. We fixed the correspondent paragraph.

3.- Is the wind field averaged over every hour?

The wind field obtained from WRF simulations contains instantaneous wind values every hour.

4.- What happens to the relative contribution if just the 0 or 12 UTC is used for each month?

To answer this question we worked with the hourly output of wind from the WRF simulation for the period 2007-2012. We selected the zonal and meridional wind components (10 m) at 0 UTC and 12 UTC, and with this information Ekman pumping was calculated.

Afterward, an average for the spring season was obtained from wind information and Ekman pumping from October and November (during this period the most intense winds are observed, specially at the local coastal jet in Puna Lengua de Vaca). Daily averages were also obtained using the same procedure.

The results are shown in Figure 1. The upper panel corresponds to the wind during spring conditions taken at a) 0 UTC, b) 12 UTC and c) from daily averages. While in the lower panel Ekman pumping is shown using winds at d) 0 UTC, e) 12 UTC and f) daily averages.

Simulations show an intensification of the wind at 0 UTC, emphasizing the coastal jet at Punta Lengua de Vaca (~30.5 °S, south of Tongoy Bay), strong winds were also observed north of Punta Choros (29 °S) and south of 31°S. These characteristics of strong winds in the afternoon (local time) disappear during the morning (12 UTC). Rahn et al. (2011) propose: "Local baroclinicity (daytimes) enhances the development of the Coastal Jet that develops from the northward advection of diabatically/subsidence heated continental air over Tongoy Bay. For reference, a layer about 500 m thick and 5 K warmer that replaces the cooler air column in the morning in the southern portion of Tongoy Bay would be associated with a local surface pressure drop of ~1 hPa inducing a strong ageostrophic acceleration of the flow"

However, when we use the daily average, we can distinguish the coastal jet and high winds in Punta de Choro and south of 31°S, but with smaller magnitudes at 0 UTC. This is due to the smoothing produced by the average. On the other hand, if we look at the structure of Ekman pumping for the three cases, all showed a similar pattern near the coast, with a positive values (favorable to upwelling), but differed in their magnitude, which is greater at 0 UTC, lower at 12 UTC, and intermediate when considering the daily averages. Further away from the coast, the negative Ekman pumping occurs when considering the 0 UTC, when the daily average is used Ekman pumping is smaller, and is not observed in the case of 12 UTC

Therefore, we believe that for the purposes of this manuscript, using daily averages of wind from the WRF simulation time is valid. The observation made by the reviewer will help the discussion, especially regarding the importance of the intensification of the coastal jet in the afternoon.

5.- Are the results in spring dominated by the intense late afternoon coastal jet? This is an important aspect for interpreting the seasonal variation.

Reply was given above

6.- Interpretation of coastal wind/drop-off zone. This is a major issue and needs to be corrected/improved. Starting at the end of page 3018-3020, the interpretation of coastal wind is based off of primarily Renault et al. (2015). There is a lot of literature on coastal wind that is much more complete. Some of the earlier works are Beardsley et al. 1987 (cf. Section 3, JGR), Burk and Thompson (1996, Mon. Wea. Rev.), Haack et al. (2001, Mon. Wea. Rev.), and many, many more. Archer and Jacobson (2005 Mon. Wea. Rev.) do a much more complete treatment of vorticity generation than Renault et al. (2015).

We thank the reviewer for this suggestion. Therefore, it corrects and improves the sections including the works mentioned by reviewer

7.- Page 3020, line 5: It says that the cool SST stabilizes the air column and results in a shallower marine boundary layer. This is not correct.

Here we refer to a particular result of Renault et al. (2016) that show, based on a sensitivity analysis, that adding an SST front of 3°C over a coastal band strip of 25 km results in weaker surface wind associated with more stable and shallow marine boundary layer.

To avoid any further confusion we have reformulated this part:

"Another minor factor is the sharp coastal sea surface temperature front associated with upwelling. Renault et al (2016) show that in their sensitivity experiment adding a sharp SST front over a coastal band strip leads to weaker surface wind associated with more stable and shallow marine boundary layer. This response of wind may be due to so-called "downward mixing" mechanism (Wallace et al. (1989); Hayes et al. (1989)), which was used by many authors to explain the observed tendency of surface winds to decelerate over colder flank of the SST front and accelerate over warmer flank of the SST front (cf. Small et al (2008) and references therein): warm (cold) SST would destabilize (stabilize) the PBL and cause enhanced (reduced) vertical turbulent mixing, increasing (decreasing) downward fluxes of horizontal momentum form the faster flow above to the slower near-surface flow. Nevertheless, a large SST anomaly (by −3 C in the experiment of Renault et al., (2016)) is needed to induce a significant weakening of wind and significant additional wind drop-off. Therefore, the SST effect can be considered as secondary compared to the orography effect over the California coast."

8.- Page 3020, line 26: Perhaps leave speculation of the atmospheric forcing mechanisms out of this.

The suggestion is accepted and was remove from the text of the manuscript.

9.- Model issues: Section 2.1 has some vague parts. Was the WRF initialized just once and ran from 2007-2012?

The WRF model was implemented and integrated for 7 years (2000-2007) using the best configuration obtained in the preliminary experiments (see Question 2). The initial and Lateral Boundary Conditions (LBC) are derived from the National Centers for Environmental Prediction's (NCEP) final analysis (FNL) fields at 1ºx1º horizontal resolution and 6 hourly interval.

For each year the model was re-initialized with the FNL reanalysis every three months leaving 6 overlap days as a spin-up, the outputs during this period were excluded from the analysis. The LBCs (updated every 6 h) are prescribed over the parent domain with the depth of 5 grid-cells where simulated variables are relaxed towards the FNL solution.

The Sea Surface Temperatures (SST) is prescribed at the lower boundary (parent and inner domains) from the OSTIA daily product (Stark et al., 2007). To include the diurnal cycle we have calculated the 6-h anomalies with respect to the daily mean from the FNL SST and then added to the daily OSTIA SST. In this way we generate the 6-h lower boundary updates with the same update rate used for the LBCs (Renault et al. (2015).

That configuration was suggested by Lo et al. 2009 in order to mitigate the problems of systematic error growth in long integrations and inconsistences between the developing flow and the lateral boundary conditions.

10.- Why does the outer domain extend all the way to 10N (Fig. 1)?

Beyond the focus of the present study we are also interested in assessing the impact of the downscaled winds from the coarser domain over a regional ocean model of the Humboldt system (Dewitte et al., 2012) whose domain extends from 5ºN to 40ºS following the approach of Cambon et al. (2013), that explains the northerly extension of the parent domain.

11.- It was stated that at least six different parameters (cumulus, PBL, soil, SST forcing, land surface, and topography [how/why was that changed?]) were evaluated (3010, line 25).

Given the complex interactions between alongshore winds, topography, cloudiness, land heating and coastal upwelling in the study region (Rahn and Garreaud 2010a, b; Wood et al., 2011; Toniazzo et al., 2011) we tested the WRF model in different configurations associated to the aforementioned process and characteristics. The objective was to identify the configuration that leads to a better model representation of the near-shore surface mesoscale atmospheric circulation in the study region. A set of eight sensitivity simulations (see Figure 3) were carried out for the control period, i.e. from 1 October 2007 to 31 December 2007 corresponding to the upwelling season in north-central Chile. The results were evaluated against surface observations from meteorological automatic stations and scatterometers (QuikSCAT, ASCAT), particular attention was paid to the shoreward decrease and temporal variability of the surface wind speed near the coast.

The sensitivity experiments were divided in four sequential phases selecting progressively the best parameters for the optimal model configuration for the long period 2007-2012:

a) Parameterization and soil models: The first four experiments (see Table 1) were implemented to compare the representation of the clouds and land surface exchange processes from two combinations of parameterizations (cumulus-PBL) and soil models already used in previous studies in the SEP (Renault et al., 2011a, b; Rahn and Garreaud 2010a, b; Toniazzo et al., 2011; Renault et al. 2015a, b).
b) SST forcing: The use of high-resolution SST products derived from satellite sources to initialized WRF has been shown to improve the representation of surface parameters in coastal regions in the SEP (LaCasse et al., 2008; Renault et al., 2012ab; Toniazzo et al, 2012; Renault et al. 2015). Here we evaluated two high-resolution daily products, the OSTIA (Stark et al. 2007) and the RTG_SST (Thiébaux et al., 2003) analysis (experiments 5-6 in Table 1) these have a spatial resolution of 0.05º and 0.5º respectively.
c) Topography and Land-Use: We have incorporated the high resolution 3-arc second SRTM topography and the accurate MODIS (1-km) land use and soil categories in order to compare the results with the previous experiments implemented with the standard 30-arc second USGS topography and Land Cover (experiment 7 in Table 1).
d) The last sensitivity test (experiment 8 in Table 1) was performed with the aim of quantifying the impact of the nesting technique over the model diagnostics and the associated CPU requirements.

12.- This means that there are a lot of different 5-year runs at 36/12/4 km that were done. Was it really just a subset that was evaluated? There is no need to show all of these runs if that is really the case, but don't oversell the evaluation of model sensitivity.

Reply to this comment in the previous question.

13.- Specific model issues: Page 3010, line 7: Increasing resolution does not always translate to greater skill, and there are other issues to consider. (see Ranjha et al. 2015, Meteorol. Atmos. Phys.)

The main objectives of the atmospheric model were to generate the mesoscale surface wind patterns that influence nearshore circulation and evaluate the sensitivity of the model resolution to capture those local wind anomalies. Given the small-scale of these wind features and the influence of the orography, coastline shape and air-sea interaction the high-resolution is a necessary requirement for the model. However as you highlight increasing resolution does not always translate to greater skill so to avoid any confusion we will reformulate this part of the model description.

14.- Page 3010, line 13: Half of the model levels are below 1.5 km? Keep in mind that a good rule of thumb is that the lowest full level should be 0.990 or 0.995 if a PBL scheme is used.

The levels in the vertical are stretched to provide higher vertical resolution toward the surface, such telescopic resolution was needed to properly simulate the MBL depth over the ocean. This is a common choice in previous studies in the SEP with the WRF model (e.g. Garreaud and Muñoz, 2005; Rahn and Garreaud 2010a, b; Toniazzo et al, 2011; Renault et al 2012a, b; Rutllant et al, 2013; among others)

15.- Page 3011, line 1: What does it mean to simulate at hourly intervals? I don't think that is the time step since the integration would be unstable. Does that mean that the output is saved every hour?

We mean that all model diagnosis in our runs were stored at hourly intervals (see Figure 2), the time steps were set to 108, 36 and 12 seconds for the domains with horizontal grid spacing of 36, 12 and 4-km respectively.

To avoid a misunderstanding we have fixed the paragraph accordingly.

16.- Page 3011: Include the range of dates for WRF in all of the figure captions. Some are 2007-2012 and others are 2007-2009. It has to be clearly stated.

We agree with the reviewer's comment and clarified this issue in the figure caption and the manuscript.

17.- Other specific comments: Page 3012, line 15: Assume that it goes to zero right at the coast?

If the question is correctly understood then the reply is, it does not go to zero right at the coast.

Taking into account an approximate the total upwelling velocity as:
Wup ~= Tc/(rho*f*Lcu) + (To-Tc)/(rho*f*Ldrop)

Where:

Tc: is the alongshore wind stress at the coast
To: is the alongshore wind stress at the offshore end of the dropoff zone
f: is Coriolis parameter
Lcu: is the length of the frictional inner shelf zone where surface and bottom Ekman layers overlap.
Ldrop: is the scale of wind dropoff
Rho: is water density

If we consider that Lcu = Ldrop, then:

Wup ~=To/(rho*f*Ldrop).

The total upwelling velocity does not depend on the coastal wind stress (Tc)

18.- Page 3012, line 20: Onshore wind? This discussion has been about the decline of the meridional wind. Is that what is meant?

Yes you are correct, there was a mistake in the manuscript the text was corrected as follows:

“a marked decline coastward of meridional wind component”

19.- Page 3013, line 3: In the previous paragraph, several assumptions were made. Here, is this using the assumption of a constant gradient and that it goes to zero at the coast, or is this the actual curl computed from the model grid?

Please note that the paragraph is rather a “note” to explain some considerations regarding both mechanisms analyzed and zonal wind distribution under certain assumptions. This was added after a suggestion given by the Editor and we found it reasonable to consider

The curl was calculated from the model grid, this was mentioned in the mansucript

20.- Page 3014, line 16/Fig 3d: Since Fig. 3e only goes out to 200 km, perhaps only extend the Fig. 3d out to ~500 km. This will also make it easier to see the detail near the shore in the model. Also, caption should be "Distance from the coast (km)"

We agree with the reviewer’s comment and extended Fig. 3d until 500km, x-label was changed to “Distance from the coast” and included in the caption

21.- Page 3017, line 6: On average...not every day has equatorward wind, especially in winter.

We agree with this comment and corrected the text

22.- Page 3017, line 25: What do you mean by integrate? It looks like these are just average values in 0.25 degree bins. What wind measurement closest to the coast is it? From QuikSCAT? Is it from the WRF (not a measurement. . .)? This needs to be much clearer since it is central to your main conclusions.

The misunderstanding most likely is, because the units in Fig. 7e are wrong, it should be $m^3 s^{-1}$. The mistake was corrected

Ekman transport was meridionally integrated every 0.25° so the final units are in $m^3 s^{-1}$ as it has been done in other related studies (e.i. Pickett and Paduan (2003); Aguirre et al., 2012)

As the reviewer mentions, WRF are not measurements, we corrected this mistake and specified that Ekman transport and pumping were obtained from numerical simulations.

23.- Page 3018, line 18: The meridional variation of the relative contribution between pumping and transport is important, but is the actual ocean response dominated by processes like upwelling shadows in the Coquimbo Bay?.

Yes indeed, processes such as upwelling shadow can be important in the Bay of Coquimbo, and are affecting the temperature distribution inside the bay, especially in the southern part of the bay close to the coast, where higher temperatures are observed (and higher thermal front) compared to the lower temperature area that extends north from Punta Lengua de Vaca (Figure 10). In fact a study in the southern part of the bay system of Coquimbo by Moraga et al. (2011) shows cyclonic circulation when there are upwelling favorable winds, the circulation is attributed to the separation of oceanic flow in Punta Lengua de Vaca, which is in agreement with the process of upwelling shadow and mainly affects the area indicated above. But we think that this is not inconsistent with the effect of the wind curl in the area, which would favor upwelling north of Punta Lengua de Vaca. The oceanic response in the area clearly needs more attention and research. In the future, we think to use an ocean model forced directly with high-resolution atmospheric simulations to analyze the oceanic response to different mechanisms.

We included a paragraph in the manuscript about the effect of an upwelling shadow and the consequences to our study.

25.- Page 3021, line 14: QuickSCAT is only twice a day at most, which can also impact the average.

Correct, we included this comment in the manuscript

26.- Page 3024, line 17: Since pumping is also correlated to transport, wouldn't that also be highly correlated? It would be good to include that to not oversell the pumping-only relationship.

Yes, in fact both mechanisms are highly related to seasonal scale, as specified on page 3018, lines 5 to 10. However, both mechanisms exhibit significant differences in upwelling transport as a function of latitude, i.e. when one is intense the other is weak (Figure 7). South of 31.25 °S, both mechanisms vary more uniformly.

We agree with the comment and included in the manuscript that due to the high correlation obtained between both mechanisms within the seasonal scale we cannot infer a relationship with SST only from Ekman pumping, especially where Ekman transport dominates.

27.- Fig. 7: Would the ratio of transport to pumping make a better comparison?

We agree with this comment and included the ratio of transport to pumping.

28.- Fig. 9: Dec. in the upper left panel.

Text was corrected

FIGURE

Figure 1: Spatial distribution for spring season of wind velocity (top panel) and Ekman pumping (EP, lower panel) using WRF wind at a-d) 0 UTC, b-e) 12 UTC and c-f) daily average obtained using WRF wind at a) 0 UTC, b) 12 UTC and c) daily average. The lower panels show the Ekman pumping (EP) obtained using WRF wind at d) 0 UTC, e) 12 UTC and f) daily average.

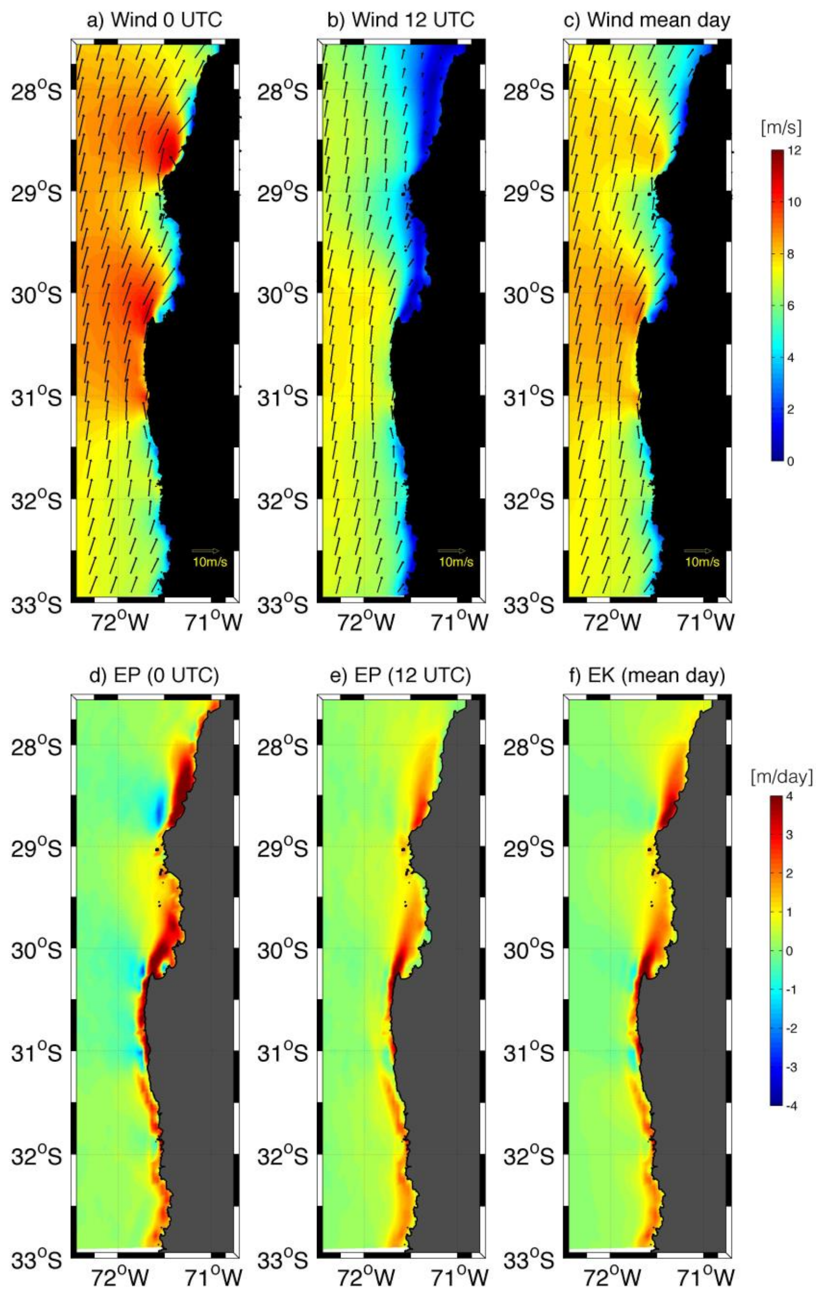

Figure 2: Schematic diagram of the experiments for the year 2007

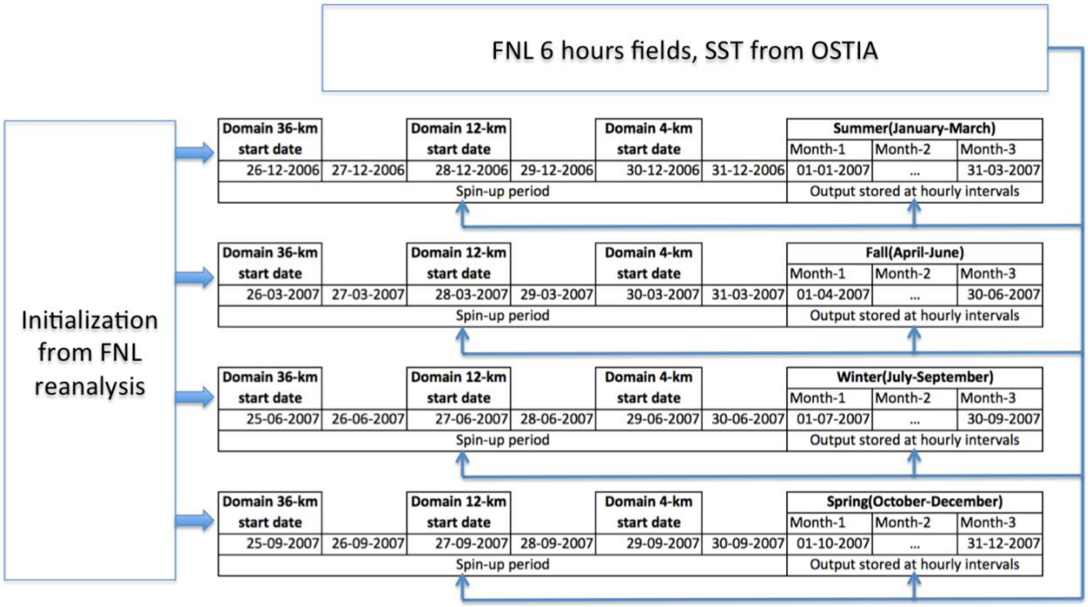

Figure 3: Different model configurations adopted for each sensitivity experiment. Shaded and bold letters highlight the selected optimal configuration.

Sensitivity phases	Nº	Convective parameterization	Planetary boundary layer (PBL)	Suface Model	SST	Nesting	Topography	Soil Categories
Parameterizations and Soil models	1	Kain-Fritsch	Mellor-Yamada-Janjic(MYJ)	Pleim-Xiu	NO SST	two-way	USGS(30'')	USGS(24) 1-km
	2	Kain-Fritsch	Mellor-Yamada-Janjic(MYJ)	NOAH	NO SST	two-way	USGS(30'')	USGS(24) 1-km
	3	Betts-Miller-Janjic(BMJ)	Bretherton and Park(UW)	Pleim-Xiu	NO SST	two-way	USGS(30'')	USGS(24) 1-km
	4	Betts-Miller-Janjic(BMJ)	Bretherton and Park(UW)	NOAH	NO SST	two-way	USGS(30'')	USGS(24) 1-km
Sea surface temperature	5	Betts-Miller-Janjic(BMJ)	Bretherton and Park(UW)	NOAH	RTG	two-way	USGS(30'')	USGS(24) 1-km
	6	Betts-Miller-Janjic(BMJ)	Bretherton and Park(UW)	NOAH	OSTIA	two-way	USGS(30'')	USGS(24) 1-km
Topography - Soil Categories	**7**	**Betts-Miller-Janjic(BMJ)**	**Bretherton and Park(UW)**	**NOAH**	**OSTIA**	**two-way**	**SRTM(3')**	**Modis(21) 1-km**
Nesting technique	8	Betts-Miller-Janjic(BMJ)	Bretherton and Park(UW)	NOAH	OSTIA	one-way	SRTM(3')	Modis(21) 1-km

RESPONSE TO REFEREE #2

We thank the reviewer for her time and constructive comments. We carefully read each of the comments and will address them as stated below:

Specific comments:

1. **Something that perturbs me is the use of the term "coastal divergence" exclusively for the Ekman Transport. Ekman transport occurs due the divergence caused by the presence of the coast, Ekman pumping occurs due the divergence in the coastal region caused by the spatial variability of the wind field. Thus, both physical processes are finally due to coastal divergence.**

   In the manuscript the term "coastal divergence" is used exclusively for the coastal upwelling due to the divergence caused by Ekman transport out of the coast and under the presence of the coast. This is different to the vertical transport that may result from the wind-stress curl, as different authors have recognized (see Graham and Largier, 1997; Capet et al., 2004; Castelao and Barth, 2006; Jacox et al., 2014)

   In general, Ekman pumping (positive) is caused by the horizontal divergence of the Ekman transport (represented by the vertical component of the cyclonic wind stress curl) without requiring a physical boundary (like the coast in the coastal upwelling or the change in f in the equatorial upwelling).

   We understand the essence of the comment that the reviewer's specifies, therefore to give the reader a better understanding we have clarified this in the manuscript.

   We propose a modification in the introduction as it follows:

   In the eastern boundary current systems wind-induced upwelling has mainly been described using two primary mechanisms. The first one is coastal divergence which is the result of offshore Ekman transport due to alongshore winds (with an equatorward component), earth's rotation and the presence of the coast (i.e. coastal upwelling).

2. **In the abstract and results, authors mention that both alongshore wind stress and wind curl show a clear seasonal variability with a marked semiannual component. Could authors propose a mechanism that produces that semiannual component?.**

   Indeed, both, atmospheric simulation and satellite observations show a semiannual variability in the along shore component of wind stress, but certainly weaker than the annual variability (Fig. 3 Annexes). In the case of the atmospheric model this is observed in Figure 4, with a secondary maximum that occurs between March and April.
   However, the mechanism that produces semiannual component is not clear to us. We have not found any study in the southeast Pacific off Chile or Peru. However, this may have some connection to the equatorial variability associated to the sun "crossing" the equator twice a year, as is presented by Li and Philander 1996 (Journal of Climate).

But nevertheless this paper indicates that although the sun "crosses" the equator twice a year, the eastern equatorial Pacific has a pronounced annual cycle in both components of surface winds. This is in contrast to the Indian Ocean and western Pacific where a semiannual oscillation of the wind is dominant on the equator".

Despite the differences between the eastern equatorial Pacific compared to the western equatorial Pacific and the Indian Ocean, as it is shown in the study of Li and Philander (1996), there is a semidiurnal component in eastern equatorial Pacific but smaller in magnitude than the annual component. Notably, the aforementioned work is based on a short observation period.

However, describing the way how this influences the southeastern Pacific off Chile is not yet evident and we think is out of the scope of this study. However, one option could be that it comes from a teleconnection similar to the mechanism that produces intraseasonal variability along our study region.

3. **In the article, the potential role of Ekman pumping on the spatial structure of sea surface temperature is also discussed. It is not clear to me why authors used one data set to force the atmospheric model (OSTIA) and another to analyze the role of Ekman pumping on SST (MUR). Please clarify.**

The use of high-resolution SST (OSTIA) products derived from satellite sources to initialized WRF has been shown to improve the representation of surface parameters in coastal regions in the SEP (LaCasse et al., 2008; Renault et al., 2012ab; Toniazzo et al, 2012; Renault et al. 2015). Here we evaluated two high-resolution daily products, the OSTIA (Stark et al. 2007) and the RTG_SST (Thiébaux et al., 2003) analysis these have a spatial resolution of 0.05º and 0.5º, respectively.

Furthermore, SST-MUR was used to compare the results obtained from Ekman pumping with the purpose of comparing the results with a different product that the one used to "force" the atmospheric model, and that also has a higher spatial resolution (~ 1 km) than OSTIA.

4. **Page 3008, line 1-5 say: "Additionally, local high frequency forcing in the region is associated with atmospheric coastal jets with period less than 25 (Garreaud and Muñoz, 2005; Muñoz and Garreaud, 2005) that are related to the variability of the South Pacific Anticyclone and play a major role in coastal upwelling (Renault et al., 2009; Aguirre et al., 2010)". I am not agree. The atmospheric coastal jets are related to synoptic dynamics of the mid-latitudes pressure perturbations (in this case high pressures) that migrate toward the east, as demonstrated by Muñoz and Garreaud, 2005 and after by Rahn and Garreaud, 2013.**

We thank the reviewer for his/her comment the text has been modified to:

"Additionally, local high frequency forcing in the region is associated with atmospheric coastal jets with period less than 25 days that are related to synoptic dynamics of the mid-latitudes pressure perturbations, in this case high pressures, that migrate toward the east (Muñoz and Garreaud, 2005; Rahn and Garreaud, 2014) and play a major role in coastal upwelling (Renault et al., 2009; Aguirre et al., 2010)"

5. **Page 3010 line 15. The reference Garreaud and Muñoz, 2005 is not correct here, due that study does not involve simulations. The correct reference should be Muñoz and Garreaud 2005, due this study involves simulations with MM5.**

   The mistake has been corrected.

6. **Page 3011 line 13 say: ". . .the results indicate a better fit in diurnal variability when model if forced with SST (OSTIA)". I wondering why you get a better fit in diurnal variability when force the model with OSTIA, if this data set lacks of a diurnal cycle, due it have daily temporal resolution as mentioned in page 3010 line 22.**

   The Sea Surface Temperatures (SST) are prescribed at the lower boundary (parent and inner domains) from the OSTIA daily product (Stark et al., 2007). To include the diurnal cycle we have calculated the 6-h anomalies with respect to the daily mean from the FNL SST and then added it to the daily OSTIA SST. Like this we generate the 6-h lower boundary updates with the same update rate used for the LBCs (Renault et al. (2015).

7. **I suggest that a final section with the summary of the major findings and conclusions should be included.**

   We agree with the reviewer's comment major findings and conclusions were included

Technical comments

Figure 3e. Due the seasonal variability of the wind stress and wind curl, it should be useful add the date of the measurements in the legend to know which line correspond to dates mention in page 3014 line 18.

We included dates in the figure and figure caption

Figure 6a. The choice of the colorbar is not adequate. Usually the drastic differentiation between reds and blues is used to distinguish between positive and negative values as in figure 6b. But the use of this colorbar in figure 6a could be confused.

Change has been made, a new colorbar using blue-red-yellow is used in Figure 6

Page 3013 line 11 say: (due upwelling). It should be (producing upwelling) ?

Text was corrected

Page 3019, line 4. Maybe the letter M is not the best choice for the Meandering index as it was used previously as Ekman transport.

We agree with the suggestion and changed the letter for Ekman transport.

Page 3023, line 28. There is a reference to the "horizontal SST gradients". It is not clear how those SST gradients were calculated. Are zonal SST gradients? Are cross-shore SST gradients? Are the maximum SST horizontal gradients? Please clarify.

The Horizontal SST gradient considers both components (zonal and meridional). We plotted the magnitude of the gradient. Text was clarified.

Page 3016 line 4 say: by astraigther coastline . . . it should be . . . by a straighter coast-line.

The mistake has been corrected

Page 3027 line 12. Reference say Jacox and Edwards, 2002. Should be Jacox and Edwards, 2012.

Reference was corrected

Seasonal variability of the Ekman transport and pumping in the upwelling system off central-northern Chile (~30°S) based on a high-resolution atmospheric regional model (WRF)

Luis Bravo[1,2,3], Marcel Ramos[2,3,1,6], Orlando Astudillo[1,4], Boris Dewitte[4,3], Katerina Goubanova[5,4]

Luis Bravo 6-8-2016 22:45
Con formato: Inglés (americano)

[1]Centro de Estudios Avanzado en Zonas Áridas (CEAZA), Coquimbo, Chile.
[2]Departamento de Biología, Facultad de Ciencias del Mar, Universidad Católica del Norte, Coquimbo, Chile.
[3]Millennium Nucleus for Ecology and Sustainable Management of Oceanic Islands (ESMOI), Coquimbo, Chile.
[4]Laboratoire d'Etudes en Géophysique et Océanographie Spatiales (LEGOS), Toulouse, France.
[5]Centre Européen de Recherche et de Formation Avancée en Calcul Scientifique (CERFACS), Toulouse, France.
[6]Centro de Innovación Acuícola Aquapacífico, Coquimbo, Chile
Corresponding author: luis.bravo@ucn.cl (L. Bravo), marcel.ramos@ucn.cl (M. Ramos)

Abstract

Two physical mechanisms can contribute to coastal upwelling in eastern boundary current systems, offshore Ekman transport due to the predominant along-shore wind stress and Ekman pumping due to the cyclonic wind stress curl, mainly caused by the abrupt decrease in wind stress (drop-off) in a cross-shore band of 100 km. This wind drop-off is thought to be an ubiquitous feature in coastal upwelling systems and to regulate the relative contribution of both mechanisms. It has been poorly studied along the central-northern Chile region because of the lack in wind measurements along the shoreline and of the relatively low-resolution of the available atmospheric reanalysis. Here, the seasonal variability in Ekman transport, Ekman pumping and their relative contribution to total upwelling along the central-northern Chile region (~30ºS) is evaluated from a high-resolution atmospheric model simulation. As a first step, the simulation is validated from satellite observations, which indicates a realistic representation of the spatial and temporal variability of the wind along the coast by the model. The model outputs are then used to document the fine scale structures in the wind stress and wind curl in relation with the topographic features along the coast (headlands and embayments). Both wind stress and wind curl had a clear seasonal variability with annual and semiannual components. Alongshore wind stress maximum peak occurred in spring, second increase was in fall and minimum in winter. When a threshold of -3x10^{-5} s^{-1} for the across-shore wind curl was considered to define the region from which the winds decrease toward the coast, the wind drop-off length scale varied between 8 and 45 km. The relative contribution of Ekman transport and Ekman pumping to the vertical transport along the coast, considering the estimated wind drop-off length, indicated meridional alternation between both mechanisms, modulated by orography and the intricate coastline. Roughly, coastal divergence predominated in areas with low orography and headlands. Ekman pumping was higher in regions with high orography and the presence of embayments along the coast. In the study region, the vertical transport induced by coastal divergence and Ekman pumping represented 60% and 40% of the total upwelling transport, respectively. The potential role of Ekman pumping on the spatial structure of sea surface temperature is also discussed.

Luis Bravo 25-7-2016 10:52
Eliminado: R

Luis Bravo 25-7-2016 14:58
Eliminado: proper

Luis Bravo 6-8-2016 21:43
Eliminado: marked

Luis Bravo 25-7-2016 10:52
Eliminado: on-shoreward

Keywords: drop-off, wind curl, upwelling, Ekman pumping

Luis Bravo 6-8-2016 22:45
Con formato: Fuente: (Predeterminado) Times New Roman

1. Introduction

In the eastern boundary current systems wind-induced upwelling has mainly been described using two primary mechanisms (Sverdrup et al., 1942; Gill 1982; Pickett and Paduan, 2003; Capet et al., 2004; Jacox and Edwards, 2012). The first one is coastal divergence which is the result of offshore Ekman transport due to alongshore winds (with an equatorward component) and earth's rotation and the presence of the coast (i.e. coastal upwelling). The second one is Ekman pumping which is the result of a cyclonic wind stress curl caused mainly by the wind drop-off that extends only tens of km in width along the coast, and is a typical feature of the eastern boundary current systems (Bakun and Nelson, 1991; Pickett and Paduan, 2003; Capet et al., 2004; Jacox and Edwards, 2012). Starting in the mid 1970s, a series of studies began assessing the contribution of Ekman pumping on coastal upwelling for the California Current System (Halpern, 1976; Nelson, 1977), which later expanded to the other four upwelling systems (Bakun and Nelson, 1991). In one of these four regions, the coast of north and central Chile, this mechanism has been poorly evaluated, primarily due to the scarcity of *in situ* data, limitations in diffusiometer winds that have a "blind zone" near the coast and the relatively low spatial resolution of the atmospheric reanalysis. This has caused a limited progresses in the understanding of the upwelling dynamics and the coastal circulation of the region, among other factors.

Coastal upwelling has been widely studied in several regions of the world, in particular along the Eastern Boundary Upwelling Systems (EBUS). Currently, there is no generalized conceptual model for the upwelling structure that considers the region near the coast, the coastal boundary and the open ocean (Mellor, 1986; Marchesiello and Estrade, 2010). Traditionally a simple relationship based on wind stress along the coast has been used as an index of the coastal upwelling intensity (Bakun, 1973), this approximation does not consider other more complex physical processes, such as the wind curl (Pickett and Paduan, 2003; Capet et al., 2004; Jacox and Edwards, 2012) and the geostrophic flow toward the coast, which is in balance with the along shore pressure gradient and could potentially limit upwelling (Marchesiello et al., 2010; Marchesiello and Estrade, 2010). In the case of the wind curl, several modeling studies from different

Luis Bravo 6-8-2016 22:45
Con formato: Fuente: (Predeterminado) Times New Roman

Luis Bravo 25-7-2016 10:54
Eliminado: ribbons

Luis Bravo 6-8-2016 22:45
Con formato: Fuente: (Predeterminado) Times New Roman

Luis Bravo 6-8-2016 22:45
Con formato: Fuente: (Predeterminado) Times New Roman

Luis Bravo 6-8-2016 22:45
Con formato: Fuente: (Predeterminado) Times New Roman

Luis Bravo 6-8-2016 22:45
Con formato: Fuente: (Predeterminado) Times New Roman

Luis Bravo 6-8-2016 22:45
Con formato: Fuente: (Predeterminado) Times New Roman

Luis Bravo 25-7-2016 10:55
Eliminado: R

Luis Bravo 6-8-2016 22:45
Con formato: Fuente: (Predeterminado) Times New Roman

Luis Bravo 25-7-2016 10:55
Eliminado: e

Luis Bravo 6-8-2016 22:45
Con formato: Fuente: (Predeterminado) Times New Roman

Luis Bravo 25-7-2016 10:55
Eliminado: This has

Luis Bravo 6-8-2016 22:45
Con formato: Fuente: (Predeterminado) Times New Roman

Luis Bravo 6-8-2016 22:45
Con formato: Fuente: (Predeterminado) Times New Roman

Luis Bravo 6-8-2016 22:45
Con formato: Fuente: (Predeterminado) Times New Roman

Luis Bravo 6-8-2016 22:45
Con formato: Fuente: (Predeterminado) Times New Roman

upwelling systems suggest that wind stress decreases within a narrow coastal band of 10-80 km called wind "drop-off" (Capet et al., 2004; Bane et al., 2005; Perlin et al., 2007; Renault et al., 2012; Renault et al., 2015) that is highly sensitive to the resolution of the model. Thus, regional ocean modeling studies show that the upwelling response is sensitive to the transition in the structure of the wind near the coast (Capet et al., 2004; Jacox and Edwards, 2012), where the structure and physical forcing of the transitional coastal wind profile is not well understood (Jin et al., 2009). In the literature at least three main hypotheses have been proposed to explain the decrease of onshore wind (drop-off) that generates the wind stress curl within the coastal band. The first is related to the change of surface and boundary layer friction in the land-sea interface (Capet et al., 2004). The second is related to the ocean-atmosphere coupling between the sea surface temperature (SST) and the wind (Chelton et al., 2007), particularly cold water upwelling tend to stabilize the atmospheric boundary layer, decoupling the high atmospheric circulation with the surface circulation. The last one is related to coastal orography (Edwards et al., 2001), coastline shape (Perlin et al., 2011), and the combination of both (Renault el at., 2015) constraining the vorticity budget of the low-level atmospheric circulation. Other possible mechanisms that could potentially contribute to wind drop-off near the coast are the effects of sea breeze and pressure gradients (across or along the coast) at sea level.

The central-northern Chile region is characterized by nutrient rich cold surface waters, attributed to the surface circulation of the Humboldt system and mainly coastal upwelling driven by along shore winds that are associated with the southeast Pacific anticyclone (Shaffer et al., 1999; Halpern, 2002). A strong seasonal variability of the southeast Pacific anticyclone produces favorable upwelling winds to peak during spring and summer and decrease during winter (Strub et al., 1998). Within central-northern Chile the area around 30°S is characterized by the most intense upwelling favorable winds (Shaffer et al., 1999; Rutllant and Montecino, 2002). Additionally, local high frequency forcing in the region is associated with atmospheric coastal jets with periods less than 25 days, that are related to synoptic dynamics of the mid-latitude pressure perturbations in this case high pressures, that migrate toward the east (Muñoz and Garreaud, 2005; Rahn and

Luis Bravo 25-7-2016 10:55
Eliminado: ,

Luis Bravo 6-8-2016 22:45
Con formato: Fuente: (Predeterminado) Times New Roman

Luis Bravo 25-7-2016 10:56
Eliminado: very

Luis Bravo 6-8-2016 22:45
Con formato: Fuente: (Predeterminado) Times New Roman

Luis Bravo 25-7-2016 10:56
Eliminado: very

Luis Bravo 6-8-2016 22:45
Con formato: Fuente: (Predeterminado) Times New Roman

Luis Bravo 6-8-2016 22:45
Con formato: Fuente: (Predeterminado) Times New Roman

Luis Bravo 6-8-2016 22:45
Con formato: Fuente: (Predeterminado) Times New Roman

Luis Bravo 25-7-2016 15:03
Eliminado: .

Luis Bravo 6-8-2016 22:45
Con formato: Fuente: (Predeterminado) Times New Roman

Luis Bravo 6-8-2016 22:45
Con formato: Fuente: (Predeterminado) Times New Roman

Luis Bravo 6-8-2016 22:45
Con formato: Fuente: (Predeterminado) Times New Roman

Garreaud, 2013) and play a major role in coastal upwelling (Renault et al., 2009, 2012; Aguirre et al., 2012). All these features make the region a natural laboratory to explore the forcing mechanisms and describe the physical processes that modulate coastal upwelling.

In a recent modeling study Renault et al. (2012) analyzed the main physical processes that explain changes in sea surface temperature in an upwelling event during the occurrence of an atmospheric coastal jet along the central-northern Chile region. The results showed a clear drop-off of the coastal wind that was not observed in the QuikSCAT data, due to the "blind zone" in the satellite measurements (~25 km offshore). The oceanic response to the atmospheric coastal jet produced significant cooling of the sea surface that significantly contributed to ocean vertical mixing equivalent to the magnitude of the vertical advection near the coast. Their sensitivity analyses showed that the response of the coastal ocean highly depends on the representation of the wind drop-off. This is because the total upwelling (*i.e.* the sum of coastal upwelling and Ekman pumping) depends on the scale of the wind drop-off. The authors suggest that there is a negative effect on coastal upwelling, due to a reduced Ekman transport near the coast that is not balanced by Ekman pumping. In addition, the drop-off has a strong effect on vertical mixing and consequently the cooling of the coastal ocean. In a previous modeling study Capet et al. (2004) off the coast of California suggested that a poor representation of the wind drop-off could underestimate Ekman pumping and overestimate coastal upwelling (and vice versa), with consequences for the coastal circulation processes. Meanwhile, Garreaud et al. (2011) using observations found a local atmospheric coastal jet just north of one of the most prominent geographic points of the region: Punta Lengua de Vaca (see Fig. 1). This coastal jet shows a distinct daily cycle as the result of the strong baroclinicity due to heating differential in the region. In a later study Aguirre et al. (2012) using climatological QuikSCAT winds to force a regional ocean model, found the importance of the wind stress curl over the regional circulation exerting control over the seasonal cycle of an Equatorward coastal jet. This study also evaluated the contribution of Ekman pumping to the total upwelling, which was not well resolved due to a poor resolution of the satellite winds within the first 30 km near the coast. In particular, due to

Luis Bravo 6-8-2016 23:32
Eliminado: 4

Luis Bravo 6-8-2016 22:45
Con formato: Fuente: (Predeterminado) Times New Roman

Luis Bravo 6-8-2016 22:45
Con formato: Fuente: (Predeterminado) Times New Roman

Luis Bravo 25-7-2016 15:04
Eliminado: passage

Luis Bravo 25-7-2016 15:04
Eliminado: a

Luis Bravo 25-7-2016 10:57
Eliminado: presents

Luis Bravo 25-7-2016 15:05
Eliminado: an

the narrow continental shelf off central-northern Chile, the cells of upwelling due to coastal divergence are trapped near the coast (Estrade et al., 2008), consequently the use of QuikSCAT winds could be overestimating the effect of upwelling driven by coastal divergence and Ekman pumping.

Although previous studies have documented the importance of the wind stress curl near the coast of central Chile (Renault et al, 2012; Aguirre et al, 2012), the impact of the abrupt transition of the wind near the coast (*i.e.* drop-off) and its seasonal variability on upwelling are still poorly understood. Here, prior to addressing this issue from an oceanic perspective, our objective is to document the wind stress curl (drop-off) and its seasonal variability off central-northern Chile (~30°S) using a high resolution (~4 km) atmospheric model. Our focus in on the Ekman pumping and its contribution to the total upwelling, and the factors that could contribute to its meridional variability (*i.e.* topography, coastline and air-sea interactions).

Luis Bravo 25-7-2016 10:57
Eliminado: is

The paper is organized as follow: a description of the atmospheric simulations and the methods used to estimate different upwelling terms are described in section 2. The following section presents results and discussions and was subdivided into three subsections. The first one describes wind stress curl pattern and the spatial scale of the wind drop-off. The second one presents an analysis of the annual variability in Ekman Pumping and coastal divergence, their relationship with coastal topography and their contribution to upwelling transport. Third one, the study relates Ekman Pumping transport to sea surface temperature near the coast. Finally, section 4 presents a summary.

Luis Bravo 6-8-2016 21:47
Eliminado: Finally

2 Methods and Model Configuration

2.1 Model Output

The Weather Research and Forecasting (WRF) model version 3.3.1 (Skamarock and Klemp, 2008) was configured with three nested domains (Fig. 1) with increasing horizontal grid spacing over the region of interest by a factor of 3 from on domain to the other. The largest synoptic domain covers most of South America and the eastern Pacific in a Mercator projection with a horizontal resolution of 36 km. The second domain covers the coast of north-central Chile (25°-35° S) with a horizontal resolution of 12 km. The innermost domain is centered over the Coquimbo bay system with a horizontal grid spacing of 4 km (Fig. 1). The use of such near-kilometer resolution improves the representation of complex terrain and is necessary for dynamical downscaling of near-surface wind speed climate over complex terrain (Horvath, 2012). WRF employs a terrain-following hydrostatic-pressure coordinate in the vertical, defined as eta (η) levels, here a total of 42 η levels were used in the vertical with increasing resolution toward the surface, 20 of them in the lowest 1.5 km with ~30 m in the vertical for the surface level, such telescopic resolution is a common choice in precedent studies to properly simulate the MBL depth over the ocean (Muñoz and Garreaud, 2005; Rahn and Garreaud 2013; Toniazzo et al, 2013; Renault et al 2012; Rutllant et al, 2013).

Given the complex interactions between alongshore winds, topography, cloudiness, land heating and coastal upwelling in the study region (Rahn and Garreaud 2013; Wood et al., 2011; Toniazzo et al., 2013) we have tested the WRF model in different combinations of parameterizations (cumulus - planetary boundary layer - soil model), surface data (SST forcing, topography and land surface) and nesting technique. A set of eight sensitivity simulations (for more details see response to referee #1, http://www.ocean-sci-discuss.net/os-2015-94/#discussion) was carried out for the control period, i.e. from 1 October 2007 to 31 December 2007 corresponding to the upwelling season in north central Chile. The results were evaluated against surface observations from meteorological automatic stations and scatterometers (QuikSCAT, ASCAT), particular attention was paid to the shoreward decrease and temporal variability of the surface wind speed near the coast. The configuration with the best estimates of observed surface variability and mean state was then used for the long simulation 2007-2012.

The initial and Lateral Boundary and Conditions (LBC) were derived from the National Centers for Environmental Prediction (NCEP) Final Analysis Data (FNL) (Kalnay et al. 1996; available online at http://dss.ucar.edu/datasets/ds083.2/) at 1°x1° global grids every six hours. The boundary conditions are prescribed over the coarser domain with the depth

luis 4-8-2016 11:10
Eliminado: see Table 1

Luis Bravo 4-8-2016 19:39
Eliminado: in

Luis Bravo 6-8-2016 22:45
Con formato: Resaltar

Luis Bravo 4-8-2016 19:39
Eliminado:

Luis Bravo 6-8-2016 22:45
Con formato: Inglés (americano)

of 5 grid-cells where simulated variables are relaxed towards the FNL solution. The SST forcing data are based on the daily Operational Sea Surface Temperature and Sea Ice Analysis (OSTIA) at 0.05°x0.05° global grids resolution (Stark et al. 2007). The Sea Surface Temperatures (SST) is prescribed at the lower boundary (parent and inner domains) from the OSTIA daily product (Stark et al., 2007). To include the diurnal cycle we have calculated the 6-h anomalies with respect to the daily mean from the six hours FNL SST and then added to the daily OSTIA SST. In this way we generate the 6-h lower boundary updates with the same update rate used for the LBCs as Renault et al. 2015.

For each year the model was re-initialized with the FNL reanalysis every three months leaving 6 overlap days as a spin-up, the outputs during this period were excluded from the analysis, this scheme was suggested by Lo et al. (2008) in order to mitigate the problems of systematic error growth in long integrations and inconsistences between the flow developing and the lateral boundary conditions. The instantaneous model diagnosis were stored at hourly intervals, the time steps were set to 108, 36 and 12 seconds for the domains of 36, 12 and 4 km respectively.

The simulated winds were validated using QuikSCAT and observations from two weather stations near the coast in Loma de Hueso (LDH) and Punta Lengua de Vaca (PLV) and a third station farther inland named Parral Viejo (Fig. 1 and 2). A spatial comparison was done using the coarse resolution grid (36 km) between satellite and WRF winds for 2007-2009. The comparison showed a good agreement between observations and modeling results with a similar spatial structure and magnitudes of the same order, especially within the study region (27ºS-33ºS). The root mean square (RMS) of the difference for observations and model results was less than 1 m s^{-1} (Fig. 2c). The high-resolution model outputs (4 km) were also compared with available observations. Initially, for each of the weather stations daily wind cycles were compared with simulations (not shown). The results indicate a better fit in diurnal variability when the model is forced with SST (OSTIA), which was finally chosen for the simulations performed in this study. The best fit between observations and model outputs was found when the wind intensifies during the afternoon between 17 and 19 hrs. A good model representation of the

Luis Bravo 6-8-2016 22:45
Con formato: Superíndice

afternoon winds is key for a proper representation of coastal upwelling in the region. Finally, for each weather station, linear regressions and dispersion plots were done between the meridional component of simulated (4 km) and observed winds (Fig. 2d-f). A good agreement was observed for all the cases.

2.2 Upwelling estimates

The relative importance of coastal upwelling due to coastal divergence (Smith, 1968) was estimated using wind stress obtained by the WRF model:

$$Et = \frac{1}{\rho_w f} \tau \times \hat{k} \qquad (1)$$

where Et is Ekman transport (m^2 s^{-1}), τ is the wind stress at the land-sea margin (~4 km from the coast), ρ_w is water density, f is the Coriolis parameter and k is a unit vertical vector. The vertical velocity from Ekman pumping was estimated using a definition given by Halpern (2002) and Renault et al. (2012).

$$w_{EP} = \frac{Curl(\vec{\tau})}{\rho_w f} + \frac{\beta \tau_x}{\rho_w f^2} \qquad (2)$$

where $\tau(x,y)$ is wind stress, β is the Coriolis parameter gradient and τ_x is the cross-shore wind stress. Latitude variations were not significant therefore the last term in equation (2) was neglected. In order to compare the two upwelling processes, Ekman pumping was converted into transport by integrating the vertical velocity within a certain distance from the coast, which in our case was the length scale of the wind drop-off (Ld) obtained from a reference value (defined by Renault et al., 2015) where cross-shore wind curl was < -3×10^{-5} s^{-1}. The wind drop-off spatial length (Ld) varies meridionally (Fig. 3d-c).

Note that if we assume that the wind is parallel to the coast and that the wind curl is dominated by its cross-shore gradient component (and this gradient is nearly constant in the drop-off zone), then the total upwelling transport is simply $\tau/(\rho f)$ or expressed as vertical velocity is $W = \tau/(\rho f Ld)$, where τ is the wind stress at Ld. Consequently it is

Luis Bravo 25-7-2016 14:40
Eliminado: The Weather Research and Forecasting (WRF) model version 3.3.1 [Skamarock and Klemp, 2008] was implemented in a configuration with three nested grids (Fig. 1) increasing the spatial resolution over the region of interest, the use of multiple grid nesting improves the representation of complex terrain and associated processes and has been found to increase the simulation skill of WRF (Horvath 2012). ... [1]

Luis Bravo 6-8-2016 22:45
Con formato: Inglés (americano)

Luis Bravo 6-8-2016 22:45
Con formato: Inglés (americano)

Luis Bravo 6-8-2016 23:19
Eliminado:

Luis Bravo 6-8-2016 22:45
Con formato: Inglés (americano)

Luis Bravo 25-7-2016 10:58
Eliminado: de la costa)

Luis Bravo 6-8-2016 22:45
Con formato: Inglés (americano)

Luis Bravo 6-8-2016 21:56
Eliminado: tangent to the local coastline

Luis Bravo 7-8-2016 21:17
Eliminado:

Luis Bravo 6-8-2016 23:04
Eliminado:

Luis Bravo 6-8-2016 23:19
Eliminado:

Luis Bravo 6-8-2016 22:45
Con formato: Inglés (americano)

Luis Bravo 6-8-2016 22:45
Con formato: Inglés (americano)

Luis Bravo 6-8-2016 22:45
Con formato: Inglés (americano)

apportioned to Ekman transport and pumping according to the amount of drop-off (for more details see Renault et al., 2012). On the other hand, in our study region there is a marked decline toward the coast of the meridional wind component, therefore the wind drop-off has an impact on the total upwelling velocity. Thus a proper assessment of scales involved in both mechanisms is crucial to the upwelling problem.

Luis Bravo 25-7-2016 10:59
Eliminado: zone

Luis Bravo 25-7-2016 10:59
Eliminado: coastward

Luis Bravo 6-8-2016 22:45
Con formato: Inglés (americano)

3 Results and discussion

3.1 Mean wind stress curl and the wind drop-off spatial scale

From the wind stress simulations (model wind outputs) we obtained the mean of the wind stress curl in the three model domains with spatial resolutions of 36, 12 and 4 km (Fig. 3a-c). The mean wind stress curl patterns show clear differences when resolution is increased. In the simulations of higher resolution small scale or finer structures are well defined, especially close to the coast, that are not present in the simulation of coarse resolution, and that are not resolved or studied in previous studies (Aguirre et al., 2012; Renault el al., 2012). The simulations with higher resolution (12 and 4 km) show a cyclonic wind stress curl (negative) within the coastal band and within the Coquimbo bay system that is associated to a positive Ekman pumping (producing upwelling). While in the oceanic sector a less intense anticyclone wind curl predominates. The negative curl within the coastal band is the result of an onshore decay in wind intensity (drop-off) that is characteristic from EBUS systems (Capet et al., 2004; Renault et al., 2012).

In the central-northern Chile region the drop-off length scale (Ld) is between 8 and 45 km (Fig. 3b-c, segmented yellow line). When the resolution of the model is increased, the wind drop-off takes place closer to the coast and exhibits a larger meridional/latitudinal variability, with in particular a larger drop-off scale in the central region of the domain than in the region south of 30.25°S. The meridional differences at Ld could be associated to coastal orography and the shape of the coastline; this will be discussed later in section 3.3. The finer structures in the wind stress curl close to shore, cannot be determined with confidence from observations of the scatterometers of previous and current satellite missions, such as QuikSCAT and/or other satellite, because of the blind zone in measurements within the first 25 km from the shore. Note that the blind zone increases to 50 km when wind stress curl is estimated, as the result of the estimate of the spatial derivative.

Renault et al. (2012) based on atmospheric simulations (obtained with WRF) determined that the extent of the wind drop-off was ~70 km. This length was different from the one

Luis Bravo 6-8-2016 22:45
Con formato: Inglés (americano)

Luis Bravo 6-8-2016 22:45
Con formato: Fuente: (Predeterminado) Times New Roman, Inglés (americano)

Luis Bravo 6-8-2016 22:45
Con formato: Inglés (americano)

Luis Bravo 6-8-2016 22:45
Con formato: Fuente: (Predeterminado) Times New Roman, Inglés (americano)

Luis Bravo 6-8-2016 22:45
Con formato: Inglés (americano)

Luis Bravo 6-8-2016 22:45
Con formato: Fuente: (Predeterminado) Times New Roman, Inglés (americano)

Luis Bravo 6-8-2016 22:45
Con formato: Inglés (americano)

Luis Bravo 6-8-2016 22:45
Con formato: Fuente: (Predeterminado) Times New Roman, Inglés (americano)

Luis Bravo 25-7-2016 15:10
Eliminado:

Luis Bravo 25-7-2016 15:09
Eliminado: a drop-off scale is more restricted to the shore and with greater spatial structure, with greater extension

Luis Bravo 6-8-2016 22:45
Con formato: Fuente: (Predeterminado) Times New Roman, Inglés (americano)

Luis Bravo 6-8-2016 22:45
Con formato: Inglés (americano)

Luis Bravo 6-8-2016 22:45
Con formato: Fuente: (Predeterminado) Times New Roman, Inglés (americano)

Luis Bravo 25-7-2016 15:12
Eliminado: ,

Luis Bravo 25-7-2016 15:12
Eliminado: which

Luis Bravo 6-8-2016 22:45
Con formato: Fuente: (Predeterminado) Times New Roman, Inglés (americano)

Luis Bravo 6-8-2016 22:45
Con formato: Inglés (americano)

Luis Bravo 25-7-2016 15:12
Eliminado: , this

obtained in this study (which varied between 8 and 45 km), possibly because of the lower resolution used in their study. To further explain the zonal wind structure and drop-off, Figure 3d shows zonal profiles of the meridional wind of the more exposed region. The results indicate a clear decay of the wind along the coast in the three simulations (36, 12 and 4 km) that is not observed in the satellite data from QuikSCAT. It should be noted the small difference with the satellite product. As mentioned above, in the study region there is a lack of wind information within the coastal band that covers the blind zone of the satellites and that can be used for validation purpose. One of the first in situ measurements in the region were done during the field campaign CupEX (Garreaud et al., 2011). During this experiment a zonal profile of wind was measured using airborne meteorological techniques. These observations allowed detecting an atmospheric coastal jet with a marked daily cycle that extended north of Punta Lengua de Vaca towards the Coquimbo bay system.

Such a coastal jet is present in our simulations that produce a wind curl in the bay system, which affects the circulation and coastal upwelling in the region. Other recent wind observations were collected under the scope of this study (FONDECYT Postdoctoral project 3130671), and are presented in Figure 3e. These wind observations were made with a marine weather station (AirMar) installed on a fishing boat. Measurements were made for 04/22/2014, 05/18/2014, 09/15/2014 and 10/28/2014. Although these measurements do not cover the period of the simulations, they are presented here to illustrate observed features of the zonal wind profiles in the southern region. Despite the large spatial and temporal variability of the observations, they suggest a tendency to a reduction of the along-shore winds toward the coast comparable to what is simulated by the model (Fig. 3d).

Focusing now on the model results, in our study region the atmospheric coastal jet extends from the coast for several tens of kilometers to the west, showing some nearshore maximums, like in Punta Lengua de Vaca (Garreaud and Muñoz, 2005; Muñoz and Garreaud, 2005, among others). In addition, near Punta Lengua de Vaca the atmospheric local and baroclinic jet (local origin), with a marked diurnal cycle has a maximum around 18:00 (local time) (Garraeud et al, 2011; Rahn et al, 2011). We compared the differences between using of WRF wind averaged only during afternoon hours and wind averaged

Luis Bravo 25-7-2016 11:00
Eliminado: zonal …tructure and drop ... [2]
Luis Bravo 25-7-2016 15:25
Eliminado: Note that this wind struct ... [3]
Luis Bravo 6-8-2016 22:45
Con formato ... [4]
Luis Bravo 6-8-2016 22:09
Eliminado: s…a wind curl north of… ... [5]
Luis Bravo 7-8-2016 21:34
Eliminado: 05
Luis Bravo 7-8-2016 21:34
Eliminado: 28
Luis Bravo 7-8-2016 21:34
Eliminado: 10
Luis Bravo 6-8-2016 22:45
Con formato ... [6]
Luis Bravo 7-8-2016 21:34
Eliminado: 04
Luis Bravo 7-8-2016 21:34
Eliminado: 18
Luis Bravo 7-8-2016 21:34
Eliminado: 15
Luis Bravo 7-8-2016 21:34
Eliminado: 09
Luis Bravo 6-8-2016 22:45
Con formato ... [7]
Luis Bravo 6-8-2016 22:45
Con formato ... [8]
Luis Bravo 6-8-2016 22:45
Con formato ... [9]
Luis Bravo 6-8-2016 22:45
Con formato ... [10]
Luis Bravo 6-8-2016 22:45
Con formato ... [11]
Luis Bravo 6-8-2016 22:45
Con formato ... [12]
Luis Bravo 6-8-2016 22:45
Con formato ... [13]
Luis Bravo 25-7-2016 11:01
Eliminado: on-shoreward
Luis Bravo 25-7-2016 11:02
Eliminado: Retaking
Luis Bravo 6-8-2016 22:45
Con formato ... [14]
Luis Bravo 25-7-2016 15:27
Eliminado: from previous paragraphs
Luis Bravo 6-8-2016 22:45
Con formato ... [15]
Luis Bravo 25-7-2016 11:02
Eliminado: at the…etween using of ... [16]

daily during the spring months (not shown). The simulation showed an intensification of the wind in the afternoon, emphasizing the coastal jet at Punta Lengua de Vaca (~30.5°S, south of Tongoy Bay), strong winds were also observed north of Punta Choros (29°S) and south of 31°S. However, when we used the daily averages, we can distinguish the coastal jet and high winds in Punta de Choros and south of 31°S, but with smaller magnitudes than in the afternoon. This is due to the smoothing produced by the averaging to daily mean data. On the other hand, if we look at the structure of Ekman pumping for the two cases, all showed a similar pattern near the coast, with a positive values (favorable to upwelling), but differed in their magnitude, which was greater in the afternoon. Therefore, we believe that for the purposes of this manuscript, using daily averages of wind from the WRF simulation time was valid.

3.2 Annual variability of the wind stress and Ekman pumping

The seasonal analysis of the wind stress and the Ekman pumping is based on the simulation having the highest resolution (4 km), considering the daily average from instantaneous wind values with an hourly sampling over the period between 01/01/2007 and 12/31/2012. Figure 4 presents the mean seasonal cycle of the wind stress for the study area in the coastal fringe extending 150 km from the coast. The wind stress presents a seasonal and spatial variability, with predominance of upwelling favorable winds (with equator-wards component) during all the year round, with maximum values (~0.15 N/m^2) between September and November, which is characteristic of the central-northern region of Chile (Shaffer et al., 1999, Rutllant and Montecino, 2002, Ranh and Garreaud, 2013). The seasonal variability of the wind stress determines the behavior of the coastal upwelling and primary productivity in the region. This is through two main mechanisms, the coastal divergence (by Ekman transport) and the Ekman pumping, that will be evaluated in the following section. The wind can also induce vertical mixing and in turn surface cooling; this could even be of the same order of magnitude as the vertical advection (Renault et al. 2012). In general, these mechanisms may covary in time, responding to the seasonal cycle of the wind stress; hence in a grouped statistical analysis (like SVD) it is difficult to isolate the spatio-temporal combined variability of two mechanisms without rejecting the effect of

Luis Bravo 25-7-2016 11:05
Eliminado: averages of

Luis Bravo 31-7-2016 9:13
Eliminado: figures

Luis Bravo 6-8-2016 22:08
Eliminado:

Luis Bravo 6-8-2016 22:08
Eliminado:

Luis Bravo 25-7-2016 11:06
Eliminado: t

Luis Bravo 25-7-2016 15:28
Eliminado: averag

Luis Bravo 25-7-2016 15:28
Eliminado: e

Luis Bravo 6-8-2016 22:45
Con formato: Fuente: (Predeterminado) Times New Roman

Luis Bravo 25-7-2016 11:08
Eliminado: is

Luis Bravo 25-7-2016 11:08
Eliminado: is

Luis Bravo 25-7-2016 15:30
Eliminado: every hour outputs

Luis Bravo 6-8-2016 23:42
Eliminado: 7

Luis Bravo 25-7-2016 15:34
Eliminado: s

the third. On the other hand, the model simulates well the coastal atmospheric jet observed in the zone of Punta Lengua de Vaca (~30ºS), in particular the maximum intensity during spring (Rahn and Garreaud, 2011; Rahn and Garreaud, 2013).

Close to the coast, where the satellite data have no coverage or the estimate in wind stress is uncertain (Fig. 1), a wind decay towards the coast (drop-off) is observed during practically all the calendar months of the year, with still a more pronounced tendency in the period between September and December. The horizontal gradient of the wind stress that is most intense close to the coast produces a wind curl with a clockwise rotation direction (cyclonic for the SH) generating a positive Ekman pumping favorable to the upwelling.

In addition to a non-uniform spatial distribution, the drop-off length (Ld) in the area of interest also exhibits a marked seasonal variability. Based on an atmospheric simulation in the west coast of USA, Renault et al. (2015) also suggested that the drop-off presents seasonal and spatial variability, but with an extension ranging from between 10 to 80 km. These authors propose that the drop-off dynamics of the wind is due mainly to orographic effects and the shape of the coastline, reaching a maximal reduction of the wind (~80%) when these are combined. According to these authors, the drop-off length scale of the wind in front of Chile should be approximately 30 km, less than the scale off the west coast of USA. This would result from the different shape of the Chilean coastline characterized by a straighter coastline and the reduced numbers of capes compared to the US West coast. In addition the Andes would induce a sharper onward decline of the wind (drop-off) than the mountains of the west coast of the USA (Renault et al., 2015). In the section 3.3 the length scale of the drop-off along the central-north coast of Chile will be analyzed in relation with the coastal orography and the shape of the coastline.

Despite that the drop-off extension in front of central-northern Chile (~45 km) is on average weaker than that estimated in the California currents system (Enriquez y Friehe, 1996; Renault et al., 2015), the wind-stress curl from this zonal gradient of the wind generates an Ekman pumping with a marked seasonality (Fig. 5) and positive vertical

Luis Bravo 25-7-2016 15:35
Eliminado: Through

Luis Bravo 6-8-2016 22:45
Con formato: Fuente: (Predeterminado) Times New Roman

Luis Bravo 25-7-2016 15:36
Eliminado: According to the authors, t

Luis Bravo 6-8-2016 22:45
Con formato: Fuente: (Predeterminado) Times New Roman

Luis Bravo 6-8-2016 22:45
Con formato: Fuente: (Predeterminado) Times New Roman

velocities (upward) that reach 4 m day^{-1}, similar values to that obtained by Pickett and Paduan (2003) in front of the region of the California current system.

The simulation (4 km) has allowed to depict and document the mesoscale atmospheric circulation in the first 50 km of the coast (Fig. 3), where the spatial patterns of the Ekman pumping are much more marked, especially at latitudes where there are sharp topographic changes in the coastline (Fig. 5). Thus, structures of Ekman pumping are highlighted to the north of the main headlands of the region (Punta Lengua de Vaca and Punta Choros), and experience a seasonal cycle. In addition, the Ekman pumping presents negative values (downwelling) off shore associated to an anti-cyclonic wind curl around 28.5°S and between 30°S and 31°S that reaches the greatest extent during August, while decreasing considerably in the summer months and beginning of fall (Fig. 5). The difference for the Ekman pumping between the mean spring and the rest of the seasons (*i.e.* summer, fall and winter) indicate that the spring positive pumping dominates the other, specially north of 29ºS, in the interior of the Coquimbo bay system and south of 31.5ºS (not shown).

With the objective of analyzing in more details the seasonal and spatial variability of the wind stress and its zonal gradient, three specific sectors of the study area were selected (28.5º, 30.5º and 32.5ºS), that are outside of the Coquimbo bay system (Fig. 6). As was mentioned before, the region is characterized by a marked wind stress seasonality more pronounced to the south of the study area (Fig. 6c). In general, the wind component along the coast shown a predominance of southerly winds favorable to the upwelling during all the year round, emphasizing a decrease in the wind stress towards the coast for the spring and summer months at 32.5ºS, and in summer at 28.5ºS and 30.5ºS. When estimating the zonal gradient of the wind stress taking as a reference the wind at the coast, the most intense positive gradients (due to the wind drop-off towards the coast) are obtained in a coastal band with a width smaller than 50 km, indicating that the Ekman pumping is the most effective inside the coastal band, as is evidenced in the Figures 4 and 5. On the other hand, the negative zonal gradient extent (Ekman pumping and downwelling) is greater in the sections located farther the north, at 28.5°S and 30.5°S, than in the section located at 32.5°S (Figs. 6 d, e and f), indicating that in the southern part of the study region, the

Luis Bravo 25-7-2016 15:39
Eliminado: to the surface
Luis Bravo 7-8-2016 21:35
Eliminado: /
Luis Bravo 6-8-2016 22:45
Con formato: Fuente: (Predeterminado) Times New Roman
Luis Bravo 6-8-2016 22:45
Con formato: Fuente: (Predeterminado) Times New Roman
Luis Bravo 7-8-2016 21:35
Con formato: Superíndice
Luis Bravo 6-8-2016 22:45
Con formato: Fuente: (Predeterminado) Times New Roman
Luis Bravo 25-7-2016 15:39
Eliminado: show
Luis Bravo 25-7-2016 15:39
Eliminado: Figure
Luis Bravo 25-7-2016 15:40
Eliminado: the
Luis Bravo 25-7-2016 11:10
Eliminado: interest
Luis Bravo 25-7-2016 11:11
Eliminado: interest
Luis Bravo 25-7-2016 11:11
Eliminado: presents values
Luis Bravo 25-7-2016 11:25
Eliminado: (on average of annual cycle)
Luis Bravo 25-7-2016 11:25
Eliminado: more to
Luis Bravo 25-7-2016 11:26
Eliminado: at

positive Ekman pumping region extends farther than in the zones where the wind stress is more intense seasonally close to the coast (Fig. 4).

3.3 Contributions of Ekman transport and Ekman pumping to the upwelling rate

The central-northern Chile continental shelf is very narrow and very steep so the scale of coastal divergence is <10 km (considering the theoretical framework of Estrade et al., 2008), while the scale of Ekman pumping considering Ld scale (previously defined, based on Renault et al., 2015) is ~45 km. To compare the seasonal contribution of coastal divergence and Ekman pumping to the total transport of coastal upwelling in the study region, the annual cycle of coastal divergence was obtained first by taking the wind of WRF closest to the coast (< 8 km) and meridionally integrated every 0.25° (Fig. 7e), while the annual cycle of Ekman pumping transport (from wind of WRF) was obtained by integrating the vertical velocity from the shoreline to the distance corresponding to the drop-off (Ld) value, also within 0.25° latitude bands (Fig. 7f).

The results indicate a marked annual cycle with maximum vertical transport in the spring, both induced by coastal divergence and Ekman pumping, with secondary maximum in some areas during autumn accounting for a weaker semiannual component. As expected, there is a large temporal coherency along the coast between both processes (the meridional average correlation between Ekman pumping and transport reaches 0.8), except locally at some latitudes (e.g. at 31.25°S) where there is a weak seasonal cycle in Ekman pumping (Fig. 7f) due to either a weak drop-off or a compensation effect by the zonal wind stress component. The high correlations indicate a seasonal consistency between both mechanisms, which has been previously reported in other upwelling systems (e.g. Pickett and Paduan, 2003; Renault et al., 2015). Although both mechanisms are highly correlated at seasonal timescales, they exhibit significant differences in relative magnitude as a function of latitude, *i.e.* when one is intense the other is weak. For instance, coastal divergence strongly dominates over Ekman pumping between 30.25ºS - 31.25ºS (Fig. 7d), which is the most recognized upwelling center in the region (located south of PLV), as well as the region between 28.5°S - 29.25ºS (north of Punta Choros). In those regions Ekman pumping

Luis Bravo 25-7-2016 12:32
Eliminado: is more extensive

Luis Bravo 6-8-2016 22:45
Con formato: Fuente: Times New Roman

Luis Bravo 6-8-2016 22:45
Con formato: Fuente: (Predeterminado) Times New Roman

Luis Bravo 25-7-2016 15:41
Eliminado: show

Luis Bravo 6-8-2016 22:16
Eliminado: ly

Luis Bravo 25-7-2016 13:52
Eliminado: to

Luis Bravo 25-7-2016 13:53
Eliminado: which is also the case

Luis Bravo 25-7-2016 13:53
Eliminado: e

Luis Bravo 25-7-2016 13:53
Eliminado: sectors

tends to be weaker, while predominant for the area between 29.25 - 30.25ºS, inside the Coquimbo bay system and the area between 28.0ºS - 28.75ºS, north of LDH. South of 31.25°S, both mechanisms vary meridionally more uniformly. The estimate of the meridional correlation between both mechanisms as a function of calendar month indicates that they are better related in spring and summer (~-0.72) than in winter (~0.45). Possible processes that could explain the inverse (negative) spatial relationship between the two mechanisms and its seasonal modulation are discussed below. Before continuing, we should mention that processes such as upwelling shadow can be important in the Coquimbo bay system, and would affect the temperature distribution inside the bay, especially in the southern part of the bay close to the coast, where higher temperatures are observed (and higher thermal front) compared to the lower temperature area that extends north from Punta Lengua de Vaca (Figure 10). In fact a study in the southern part of the Coquimbo bay system (Moraga et al., 2011) shows cyclonic circulation when there are upwelling favorable winds, the circulation is attributed to the separation of oceanic flow in Punta Lengua de Vaca, which is in agreement with the process of upwelling shadow and mainly affects the area indicated above. However, we think that this is not inconsistent with the effect of the wind curl in the area, which would favor upwelling north of Punta Lengua de Vaca. The oceanic response in the area clearly needs more attention and research in the future studies.

Considering the influence of topography and the geometry of the coastline to describe the spatial variability of the wind stress, (e.g. Winant et al., 1988; Burk and Thompson, 1996; Haack, et al., 2001; Koracin et al., 2004; Renault et al., 2015, among others), we now document the relationship between the relative importance of Ekman transport and pumping, and the coastal topography and shape of the coastline in the region. An along-coast orography index (H_{index}) is estimated from the average of the orographic height between the coastline and 100 km inland (as in Renault et al. 2015). In addition, the coastline meandering index (M_{index}) is estimated by converting the position of the coastline into distances and afterward using a high variability-pass filter (with 10 km half- width) the small fluctuations in the index are smoothed, consequently the index only considers the abrupt change in coastline configuration at relatively large scale (Renault et al., 2015). Figure 7a shows the H_{index} (black line) and M_{index} (red line). In the latter index negative

Luis Bravo 6-8-2016 22:45
Con formato: Fuente: (Predeterminado) Times New Roman
Luis Bravo 25-7-2016 13:54
Eliminado: ies
Luis Bravo 25-7-2016 13:55
Eliminado: ,
Luis Bravo 25-7-2016 13:55
Eliminado: more
Luis Bravo 6-8-2016 22:18
Eliminado: of Coquimbo
Luis Bravo 25-7-2016 13:56
Eliminado: by
Luis Bravo 25-7-2016 13:56
Eliminado: (
Luis Bravo 25-7-2016 15:42
Eliminado: But
Luis Bravo 25-7-2016 13:56
Eliminado: work
Luis Bravo 25-7-2016 13:57
Eliminado: Tomando en cuenta la influencia de la topografía de costa y geometría de la linea de costa sobre la variabilidad espacial del esfuerzo del viento
Luis Bravo 6-8-2016 22:19
Eliminado: entre otros
Luis Bravo 25-7-2016 13:57
Eliminado: .
Luis Bravo 25-7-2016 13:57
Eliminado: W
Luis Bravo 25-7-2016 13:58
Eliminado: along-shore
Luis Bravo 25-7-2016 13:59
Eliminado: applied to the coastal longitude
Luis Bravo 6-8-2016 22:45
Con formato: Fuente: (Predeterminado) Times New Roman

values are associated with headlands, while positive values are associated with bays. The drop-off scale and alongshore wind at the coast and at Ld are also included (Fig. 7b-c). Note that Ld is inversely proportional to coastal wind (R^2 de ~0.81), while the wind evaluated at Ld is spatially more homogenous. This differs from the results obtained by Renault et al. (2015) along the western coast of USA. From the inspection of H_{index}, M_{index} and Ld three scenarios are defined that could explain the observed upwelling pattern (Fig. 7d-f):

1. Prevalence of positive Ekman pumping: in sectors such as the Coquimbo bay system and the region north of 28.5ºS (LDH), where the wind curl intensifies due to the sharp decline of onshore wind, with a large drop-off scale (Ld). In addition, the combination of a high orography (large H_{index}) and the presence of bays and headlands along the coastline favor a decrease in the meridional onshore wind.

2. Prevalence of coastal divergence: in sectors characterized by a low topography (small H_{index}) and a negative M_{index} due to the presence of headlands such as Punta Lengua de Vaca and Punta Choros, with a drop-off scale (Ld) smaller and stronger winds alongshore (Fig. 7b-c).

3. South of 31.25°S the pattern is more complex than previous scenarios. Both mechanisms are present but with a slight dominance of coastal divergence on Ekman pumping. South of this latitude, Ld increases, coastal wind decreases and wind curl increases (Fig. 7b-c). M_{index} shows the presence of small inlets and headlands and the orography index is moderate high without largest changes as in the northern coastal region.

Renault et al. (2015) proposed that the coastal topography induces a decrease in the intensity of the wind towards the coast through the vortex stretching term. Similarly, Archer and Jacobson (2005) from atmospheric numerical simulations showed that the topography in the Santa Cruz-California region, is required for the formation of turbulence and vorticity. On the other hand, the shape of the coastline with capes and headlands increases the orographic effect through the vortex stretching term, tilting-twisting and

Luis Bravo 6-8-2016 22:21
Eliminado:

Luis Bravo 6-8-2016 22:45
Con formato: Fuente: (Predeterminado) Times New Roman, Inglés (americano)

Luis Bravo 6-8-2016 22:45
Con formato: Fuente: (Predeterminado) Times New Roman

Luis Bravo 6-8-2016 22:45
Con formato: Fuente: (Predeterminado) Times New Roman

Luis Bravo 6-8-2016 22:45
Con formato: Fuente: (Predeterminado) Times New Roman, Inglés (americano)

Luis Bravo 7-8-2016 21:37
Eliminado: orograpahy

Luis Bravo 6-8-2016 22:45
Con formato: Fuente: (Predeterminado) Times New Roman, Inglés (americano)

Luis Bravo 6-8-2016 22:45
Con formato: Fuente: (Predeterminado) Times New Roman

Luis Bravo 6-8-2016 22:45
Con formato: Fuente: (Predeterminado) Times New Roman

Luis Bravo 25-7-2016 13:59
Eliminado: Del mismo modo, Archer and Jacobson (2005) a partir de simulaciónes numéricas atmosférica demostraron que la topografia en el sector de Santa Cruz, California son necesarios para la formación de turbulencia y vorticidad. Por otro lado

Luis Bravo 25-7-2016 13:59
Eliminado: ,

turbulent flux divergence (Archer and Jacobson, 2005; Renault et al., 2015). The sea-land drag coefficient difference mainly acts as a barrier that turns the wind alongshore.

Another minor factor is the sharp coastal sea surface temperature front associated with upwelling. Renault et al (2015) show that in their sensitivity experiment adding a sharp SST front over a coastal band strip leads to weaker surface wind associated with more stable and shallow marine boundary layer. This response of wind may be due to so-called "downward mixing" mechanism (Wallace et al., 1989; Hayes et al., 1989), which was used by many authors to explain the observed tendency of surface winds to decelerate over colder flank of the SST front and accelerate over warmer flank of the SST front (*cf.* Small et al., 2008 and references therein): warm (cold) SST would destabilize (stabilize) the PBL and cause enhanced (reduced) vertical turbulent mixing, increasing (decreasing) downward fluxes of horizontal momentum form the faster flow above to the slower near-surface flow. Nevertheless, a large SST anomaly (by −3 ºC in the experiment of Renault et al., 2015) is needed to induce a significant weakening of wind and significant additional wind drop-off. Therefore, the SST effect can be considered as secondary compared to the orography effect over the California coast.

The combination of coastal topography and the presence of headlands, points and capes on the United State (US) west coast, which induces a stronger and larger wind drop-off, which in turn is associated with a positive Ekman pumping (Koracin et al., 2004; Renault et al., 2015). This characteristic differs from what is observed along central-northern Chile, where the larger drop-off (Ld) length, associated with a strong wind curl (Fig. 7b-c), takes place in the presence of abrupt orography and within the Coquimbo bay system (30.25ºS - 29.25ºS). There the cross-shore wind component is more intense and favors the wind curl, whereas with lower terrain and the presence of headlands the Ld is very small (*cf.* Fig. 10, Renault et al., 2015). The origin of these differences is not well known; they may be due to several factors or processes. For instance, the topographic terrain along the coast of northern Chile is much higher (for the coastal range and Andes mountains) than the terrain along the west coast of the US. Furthermore, a feature of particular interest north of Punta Lengua de Vaca is the presence of the local atmospheric jet, which has a strong diurnal cycle and a clear

Luis Bravo 6-8-2016 22:45
Con formato: Fuente: (Predeterminado) Times New Roman

Luis Bravo 6-8-2016 22:45
Con formato: Fuente: (Predeterminado) Times New Roman

Luis Bravo 6-8-2016 22:22
Eliminado: (1…89)… Hayes et al., ... [17]

Luis Bravo 6-8-2016 22:45
Con formato ... [18]

Luis Bravo 6-8-2016 22:23
Eliminado: (…008)…and reference ... [19]

Luis Bravo 6-8-2016 22:45
Con formato: Fuente: (Predeterminado) Times New Roman

Luis Bravo 25-7-2016 14:00
Eliminado: In a way that…his chara ... [20]

seasonal variability, as a result of coastal topography that favors baroclinicity north of PLV (Garreaud et al., 2011; Rahn et al., 2011). This feature would deserve further consideration based on the experiments done with the regional atmospheric model, however this is beyond the scope of the present study. Here the focus is on understanding possible effect of the wind drop-off and its spatial and seasonal variability on the upwelling dynamics.

To determine the contribution of the two proposed mechanisms to the total upwelling in the region, vertical transport due to coastal divergence and Ekman pumping were meridionally integrated (from Fig. 7e and 7f, respectively). The contributions of both mechanisms to upwelling (Fig. 8) have a clear annual cycle with a marked semiannual component. Maximum values occur during October, with 0.23 and 0.14 Sv for Ekman transport and Ekman pumping, respectively, while the sum of both is 0.37 Sv. In addition, coastal divergence and Ekman pumping represent 60% and 40% of the total upwelling, respectively. This indicates that Ekman transport is the stronger upwelling mechanism. However, it should be noted that these values are the sum throughout the region, and these percentages would change if specific sectors were considered especially where Ekman pumping has a larger significance (Fig. 7).

Comparing our estimates with those obtained by Aguirre et al. (2012) from QuikSCAT wind information using a larger region (~27.5°S - 40°S), it is observed that coastal divergence from our study is lower, mainly because they estimated averages using only 2 values every day, which may influence the daily mean and therefore their estimates. Also their analysis did not include the wind drop-off area. The winds used in their study are stronger and so are their estimates for coastal divergence (*cf.* Fig. 7, Aguirre et al., 2012). However, for Ekman pumping our results are only slightly smaller than theirs. This difference is mainly due to differences in the method employed to estimate the vertical upwelling transport. In particular they use a length scale (Ld) of 150 km from the coast for their calculation, while in this study a value of 45 km was considered. However, the largest differences in the estimates of the contributions of both mechanisms to total upwelling are in the seasonal variability and the relative contribution to Ekman pumping. The seasonal variability is composed of an annual cycle with a significant semiannual component,

Luis Bravo 25-7-2016 14:12
Eliminado: tion

Luis Bravo 25-7-2016 14:12
Eliminado: .

Luis Bravo 25-7-2016 14:12
Eliminado: study

Luis Bravo 25-7-2016 14:13
Eliminado: ation

Luis Bravo 25-7-2016 14:13
Eliminado: which

Luis Bravo 25-7-2016 14:14
Eliminado: different

Luis Bravo 25-7-2016 14:14
Eliminado: their data is only twice a day at most, which can also impact the average, and do

Luis Bravo 6-8-2016 22:24
Eliminado: .

whereas that obtained by Aguirre et al., (2012) is rather dominated by the annual cycle. This is because their estimates are based on the average over a larger region that includes the central-southern Chile region, where the wind has a significant annual variability. Moreover, the present results show a higher relative contribution of Ekman pumping to total upwelling in our region. This is partly due to a different technique for estimating this mechanism, the use of different wind products and the differences in the length of both study areas.

3.4 Annual variability of Ekman Pumping and its relationship with Sea Surface Temperature near the coast

A link between SST and wind is found throughout the world's ocean wherever there are strong SST fronts (see review by Xie, 2004; Chelton et al., 2007; Small et al., 2008). This link raises the questions of to what extent the wind-drop off could be associated to marked upwelling fronts in EBUS. In the context of our study, it consists in evaluating the relationship between Ekman pumping and SST, considering that the difficulty to tackle this issue is related to the fact that there is a large temporal coherence between Ekman pumping and transport, preventing a clear identification of Ekman pumping-induced SST anomalies where both processes are in phase. As an attempt to identify regions where Ekman pumping has an imprint on SST, we use the Multi - Scale Ultra - High Resolution SST data set (MUR, http://mur.jpl.nasa.gov) with a spatial resolution of 1 km, which was shown to better capture SST fronts than other products off Peru (Vazquez et al., 2013). Figure 9 shows the annual cycle of the MUR SST. The satellite data were compared to *in situ* observations that were obtained from 13 thermistors positioned close to surface along the coastline between 28ºS–32ºS (these observations were obtained by Centro de Estudios Avanzados en Zonas Aridas, Coquimbo, Chile) covering the period 09/2009–09/2012. The correlations obtained between observations and satellite data were high (0.74-0.94 most values were 0.8) and the RMS between their differences was low varying between 0.54 and 1.3°C. This provided confidence to use MUR temperatures close to the coast in the spatio-temporal analysis done in the study region. The MUR data showed that south of 28.5°S there is a persistent surface cooling through all the year that increases in length (offshore)

Luis Bravo 25-7-2016 15:44
Eliminado: they make their estimates considering

Luis Bravo 6-8-2016 22:45
Con formato: Fuente: (Predeterminado) Times New Roman

Luis Bravo 6-8-2016 22:45
Con formato: Inglés (americano)

Luis Bravo 6-8-2016 22:45
Con formato: Inglés (americano)

Luis Bravo 6-8-2016 22:26
Eliminado:

Luis Bravo 25-7-2016 15:45
Eliminado: e

Luis Bravo 25-7-2016 15:46
Eliminado: have comparable contribution

Luis Bravo 6-8-2016 22:45
Con formato: Fuente: (Predeterminado) Times New Roman

Luis Bravo 6-8-2016 22:45
Con formato: Fuente: (Predeterminado) Times New Roman

Luis Bravo 25-7-2016 15:47
Eliminado: SST results

from ~10 km in the northern region to ~100 km in the southern region. Within this region there are prominent upwelling centers, Punta Lengua de Vaca (~30.5ºS), Punta Choros (~29ºS) and the region between 30.5°S – 33°S. During most of the year a cold surface tongue projects offshore towards the great system of embayments of Coquimbo (with limits between ~29.25°S and 30.25°S), north of Punta Lengua de Vaca. A less intense but with a similar structure is observed north of Punta Loma de Hueso (~28.8ºS).

An illustration of the effect of Ekman pumping on SST is presented in Figure 10 which shows the October mean spatial distribution for wind stress, Ekman pumping, SST and SST gradient. This month was selected because the maximum values of wind stress and increased surface cooling are recorded during this period. During this month, the wind stress (Fig. 10a) was intense with maximum values of ~0.15 Nm^{-2}, showing a clear zonal gradient (drop-off) over the entire coastal band of the study area. Note that the maximum wind stress is north of the two most prominent headlands of the region (PLV and LDH), right where the wind abruptly changes direction, creating an intense cyclonic wind curl north of both ends. As the result from the distribution pattern of the wind stress, wind curl was negative in much of the area of interest resulting in a positive Ekman pumping with vertical velocities of up to 4 m day^{-1} near the coast (Fig. 10b). Also, there are two areas with a slightly negative pumping (light blue regions), following the pattern of the wind stress where the wind decreases away from the coast (see the wind vectors), producing a positive curl and a negative Ekman pumping. Moreover, as mentioned above (see Fig. 7), much of the southern spatial structure in Ekman pumping appears to be associated to the coastal terrain and abrupt changes of the coastline. A good example of this is the tongue-shaped structure that extends from the upwelled waters north of Punta Lengua de Vaca entering the Coquimbo bay system, where the upwelling induced by the Ekman transport seems not affected (Fig. 7). As the result of a positive Ekman pumping, cold water rises to surface causing a decrease in sea surface temperatures in large part of the coastal region (Fig. 10c). However, this cooling is not necessarily caused by Ekman pumping throughout the region, there are other processes that would contribute to the surface cooling that will be discussed later. Despite this, the cooling inside the Coquimbo bay system seems to be caused largely by Ekman pumping. Moreover, outside the Coquimbo bay system high

Luis Bravo 6-8-2016 22:45
Con formato: Fuente: (Predeterminado) Times New Roman

Luis Bravo 6-8-2016 22:45
Con formato: Fuente: (Predeterminado) Times New Roman

Luis Bravo 6-8-2016 22:45
Con formato: Fuente: (Predeterminado) Times New Roman

Luis Bravo 6-8-2016 22:26
Eliminado: SBC,

Luis Bravo 7-8-2016 21:37
Eliminado: y

Luis Bravo 6-8-2016 22:45
Con formato: Fuente: (Predeterminado) Times New Roman

Luis Bravo 25-7-2016 14:15
Eliminado: in

Luis Bravo 25-7-2016 15:49
Eliminado: abruptly

values (>2° C km^{-1}) of the horizontal SST gradient magnitude are distributed in a band near the coast, but not attached to it (Fig. 10d) as expected for upwelling fronts. Within the Coquimbo bay system, there is a homogeneous temperature zone, delimited by a less intense gradient in the west and a greater gradient in the smaller bays of the system, which coincides with the structure of an Ekman pumping tongue projected to the north of Punta Lengua de Vaca.

In order to further document the coupled spatio-temporal patterns of Ekman pumping and the SST field, a Singular Value Decomposition analysis (SVD, Venegas et al., 1997) was performed. The SVD method allows determining statistical modes (time/space) that maximize the covariance between two data sets. Filtered time series (low pass filter with mean half-power of 280 days) and standardized of Ekman pumping and SST-MUR for the 2007-2012 period were analyzed using this method (Fig. 11). In this case the SVD analysis was successful in capturing a dominant seasonal mode. The first dominant mode accounts for 99% of the covariance, with a 43% and 87% of the variance explained by Ekman pumping and SST respectively. Ekman pumping spatial pattern presents maximum values very close to the coast, primarily north of Punta Lengua de Vaca, inside the Coquimbo bay system (29.3ºS–30.2ºS) and north of Punta Choros (28ºS - 29ºS). Also, the pattern is intense near the coast between 30.2ºS (south of PLV) and 32.5ºS. The spatial pattern for SST presented areas with high variability associated with areas of maximum Ekman pumping, highlighting the overall variability in the bay system of Coquimbo and the area north of Loma de Hueso (~ 28.8°S). Moreover, the correlation between the time series of expansion coefficient was -0.96 (with R^2 = 0.92 and significant at 95 %), indicating a strong inverse relationship, consistent with that expected for a positive pumping with upward vertical velocities that causes a surface cooling in the region. This results in a greater contribution to the north of headlands in the region (Punta Lengua de Vaca and Loma de Hueso), even within the Coquimbo bay system, which is consistent with the results observed in Figure 7. However, despite the high correlation obtained between both mechanisms within the seasonal scale we cannot infer a relationship with SST only from Ekman pumping, especially where Ekman transport dominates. Also, other processes such as the direct effect of wind must play a significant role, eg. vertical mixing (Renault et al.,

Luis Bravo 25-7-2016 15:50
Eliminado:

Luis Bravo 25-7-2016 14:15
Eliminado: to

Luis Bravo 25-7-2016 14:15
Eliminado: e

Luis Bravo 25-7-2016 14:16
Eliminado: with

Luis Bravo 25-7-2016 15:50
Eliminado: to the surface

Luis Bravo 6-8-2016 22:45
Con formato: Fuente: (Predeterminado) Times New Roman

Luis Bravo 6-8-2016 22:28
Eliminado: of Coquimbo

Luis Bravo 25-7-2016 14:16
Eliminado: But

Luis Bravo 25-7-2016 14:16
Eliminado: a significant role must be played by other processes such as the direct effect of wind

2012), or processes related to mesoscale activity (filaments, meanders, eddies, etc.), which are more intense south of Punta Lengua de Vaca (Hormazabal et al., 2004), and/or in general processes related to ocean-atmosphere interaction (Chelton et al., 2007; Renault et al., 2015).

Finally, our analysis calls for more thorough study on the temperature response to wind forcing, which should involve oceanic modeling at a resolution high enough to resolve finer scale processes. The oceanic model could be forced by the high-resolution atmospheric simulations presented in this study, improving in terms of resolution from previous modeling efforts in the region (Renault et al., 2012). The use of a high-resolution coupled ocean-atmosphere model would improve our understanding of the air-sea interactions along our study region. A plan for the development of such model is under way and will be the focus of our next study.

4.- Summary

The spatial and temporal variability (annual cycle) of the transport and Ekman pumping, as well as their relative contribution to the total upwelling in the central-northern Chile was studied using winds obtained from a nested configuration of the WRF model allowing to reach 4-km resolution. The simulations showed a cyclonic wind curl (negative) on the coastal-band nearshore and inside the Coquimbo bay system. This negative wind curl is mainly due to the onshore decay of the wind (wind drop-off), which presented length scales (Ld) between 8 and 45 km with a significant latitudinal variability. The wind drop-off scale is in particular larger within 29.25°S-30.25°S and to the north of 28.5°S. When we compared the drop-off scale with other upwelling regions, for example the coast of California (Enriquez and Friehe., 1996; Renault et al, 2015), we find that it is lower in our study region. For instance Ld ranges from 10 and 80 km within 35°N and 45°N (Renault et al., 2015). Despite such difference, the wind stress curl that resulted from this zonal wind shear, generated Ekman pumping with a marked seasonality and vertical velocities at the surface that reached 4 m/day, values comparable to those observed in the California current system.

Luis Bravo 6-8-2016 22:29
Eliminado: Summarizing

Luis Bravo 6-8-2016 22:45
Con formato: Fuente: (Predeterminado) Times New Roman

Luis Bravo 25-7-2016 14:18
Eliminado: comparable

Luis Bravo 25-7-2016 14:18
Eliminado: for the

Luis Bravo 25-7-2016 15:51
Eliminado:

Luis Bravo 25-7-2016 14:19
Eliminado: coupled

Luis Bravo 25-7-2016 14:19
Eliminado: c

Luis Bravo 25-7-2016 14:19
Eliminado: be also a step further for improving

Luis Bravo 25-7-2016 15:52
Eliminado: ocean-atmosphere

Luis Bravo 25-7-2016 14:21
Eliminado: in this

Luis Bravo 25-7-2016 14:22
Eliminado: This is planned for future work.

Luis Bravo 6-8-2016 22:45
Con formato: Fuente: (Predeterminado) Times New Roman

When comparing the seasonal contribution of coastal divergence and Ekman pumping to the coastal upwelling transport in northern-central Chile, we find that there is a high seasonal coherence between the two mechanisms (> 0.8) with a maximum during spring. However, despite this high seasonal correlation there is a spatial alternation between them, that is, where one is intense the other is weak. This pattern seems to be the result of a close relationship between the topography of the coast, the shape of the coastline and the spatial scale of the wind drop-off. From this information we defined three scenarios that could explain the pattern of upwelling in the area.

Prevalence of positive Ekman pumping associated to large of Ld, observed in regions such as the Coquimbo bay system and north of 28.5ºS. The combination of high terrain and the presence of bays and headlands along the coastline could explain the large Ld values.

Prevalence of coastal divergence with smaller values of Ld and more intense winds near the coast. This is observed in sectors characterized by a low topography and the presence of headlands as Punta Lengua de Vaca and Punta Choros.

Luis Bravo 6-8-2016 23:18
Con formato: Sangría: Izquierda: -0,63 cm

Combination of both mechanisms where neither divergence nor coastal Ekman pumping dominated over the other. This take place to the south of 31.5°S.

Luis Bravo 6-8-2016 23:18
Con formato: Sangría: Izquierda: -0,63 cm

The 3-dimensional aspect of the coastal circulation in the region of interest (Aguirre et al., 2012) prevents a clear identification of the role of each processes on SST variability, although our SVD analysis reveals areas where the similarity of the patterns of Ekman pumping and SST suggests a privileged forcing mechanism like within the Coquimbo bay system and the area north of Loma de Hueso (~ 28.8 °S). Further studies based on the experimentation with an regional oceanic model should be carried out to better identified upwelling regimes by, for instance, using the model winds documented here at different seasons to mimic changes in the drop-off. Considering the rich marine ecosystem hosted by the region (Thiel et al., 2007), our interest goes to relate aspects of the meso to submeso scale circulation (eddies and filaments) to the processes documented in this study. This is planned for future work.

Luis Bravo 6-8-2016 23:55
Eliminado:

Finally, the model allowed for an estimate of the near-shore (coastal frange of ~50km) low-level circulation and, evidences fine scale structure of the wind stress curl that cannot be estimated from satellite observations. Considering the overall realism of the model simulation, our study could be used to guide field experiments and gather in situ measurements in order to gain further knowledge in the processes that constrain such features

Acknowledgements

This work was financed by Postdoctoral FONDECYT/Chile Nº 3130671 and support from Centro de Estudios Avanzados en Zonas Aridas (CEAZA), Coquimbo, Chile. M. Ramos, L. Bravo and B. Dewitte acknowledge support from FONDECYT (project 1140845) and Chilean Millennium Initiative (NC120030). B. Dewitte and M. Ramos acknowledge support from FONDECYT (project 1151185). CNES (Centre National d'Etudes Spatiales, France) is thanked for financial supports through the OSTST project EBUS-South. Katerina Goubanova was supported by IRD. The contribution from two reviewers and the editor is deeply appreciated; their comments and suggestions improved and strengthen this study

Luis Bravo 6-8-2016 22:45
Con formato: Inglés (americano)

Luis Bravo 6-8-2016 23:18
Con formato: Justificado, EspacioPosterior: 0 pto, Interlineado: 1,5 líneas

luis 4-8-2016 11:12
Eliminado: .

Luis Bravo 6-8-2016 22:45
Con formato: Inglés (americano)

Luis Bravo 6-8-2016 22:45
Con formato: Sin Resaltar

Luis Bravo 6-8-2016 22:45
Con formato: Inglés (americano)

5.- References

Aguirre, C., Pizarro, O., Strub, P. T., Garreaud, R. and Barth, J.A.: Seasonal dynamics of the near-surface alongshore flow off central Chile, J. Geophys. Res., 117, C01006, doi:10.1029/2011JC007379, 2012.

Archer, C. L. and Jacobson, M. Z.: The Santa Cruz Eddy. Part II: Mechanisms of Formation, Mon. Weather Rev., 133(8), 2387–2405, doi:10.1175/MWR2979.1, 2005.

Bakun, A.: Coastal upwelling indices, west coast of North America, 1946-71. U.S.Dep. Commer., NOAA Tech. Rep., NMFS SSRF-671, 103 p., 1973.

Bakun, A. and Nelson, C.: The seasonal cycle of wind stress curl in subtropical Eastern boundary current regions. J. Phys. Oceanogr., 21: 1815-1834, 1991.

Bane, J. M., Levine, M. D., Samelson, R. M., Haines, S. M., Meaux, M. F., Perlin, N., Kosro, P. M. and Boyd, T.: Atmospheric forcing of the Oregon coastal ocean during the 2001 upwelling Season, J. Geophys. Res., 110.C10S02, 2005.

Beljaars, A.C.M.: The parameterization of surface fluxes in large-scale models under free convection. Quart. J. Roy. Meteor. Soc., 121, 255–270, 1994.

Bretherton, C. S. and Park, S.: A new moist turbulence parameterization in the Community Atmosphere Model. J. Climate, 22, 3422–3448, 2009.

Burk, S. D. and Thompson, W. T. : The summertime low-level jet and marine boundary layer structure along the California coast. Mon. Weather Rev., 124, 668–686, 1996.

Capet, X. J., Marchesiello, P. and McWilliams, J. C.: Upwelling response to coastal wind profiles, Geophys. Res. Lett., 31, L13311, 2004.

Chelton, D. B., Schlax, M. G. and Samelson, R. M.: Summertime coupling between sea surface temperature and wind stress in the California Current System, J. Phys. Oceanogr., 37, 495-517, 2007.

Dyer, A. J. and Hicks, B. B.: Flux–gradient relationships in the constant flux layer. Quart. J. Roy. Meteor. Soc., 96, 715–721, 1970

Edwards K.A., Rogerson A.M., Winant C.D. and Rogers D.P.: Adjustment of the marine atmospheric boundary layer to a coastal cape, J Atmos Sci 58(12):1511–1528, 2001.

Enriquez, A.G. and Friehe, C.A. : Effects of Wind Stress and Wind Stress Curl Variability on Coastal Upwelling J. Phys. Oceanogr., 25, 1651-1671, 1996.

Estrade, P., Marchesiello, P., Colin de Verdiere, A. and Roy, C.: Cross-shelf structure of coastal upwelling: A two-dimensional expansion of Ekman's theory and a mechanism for

Luis Bravo 6-8-2016 23:11
Con formato: Fuente: Times New Roman

Luis Bravo 25-7-2016 15:54
Eliminado: 4

Luis Bravo 6-8-2016 23:11
Con formato: Fuente: (Predeterminado) Times New Roman, Inglés (americano)

Luis Bravo 6-8-2016 23:10
Con formato: Interlineado: sencillo

Luis Bravo 6-8-2016 23:11
Con formato: Inglés (americano)

Luis Bravo 6-8-2016 23:11
Con formato: Fuente: Times New Roman

Luis Bravo 6-8-2016 23:11
Con formato: Fuente: (Predeterminado) Times New Roman, Inglés (americano)

Luis Bravo 6-8-2016 23:11
Con formato: Fuente: Times New Roman

inner shelf upwelling shut down, J. Mar. Res., 66, 589–616, doi:10.1357/002224008787536790, 2008.

Garreaud, R. and Muñoz, R.: The low-level jet off the subtropical west coast of South America: Structure and variability, Mon. Weather Rev., 133, 2246–2261, doi:10.1175/MWR2972.1, 2005.

Garreaud R, Rutllant, J., Muñoz, R., Rahn, D., Ramos, M. and Figueroa, D.: VOCALS-CUpEx: The Chilean Upwelling Experiment, Atmos. Chem. Phys., 11, 2015–2029, doi:10.5194/acp-11-2015-2011, 2011.

Gill, A.E.: Atmosphere–ocean dynamics, International Geophysics Series 30, 403pp, 1982.

Haack, T., Burk, S. D., Dorman, C. and Rogers, D.: Supercritical Flow Interaction within the Cape Blanco–Cape Mendocino Orographic Complex, Mon. Weather Rev., 129, 688–708, 2001.

Halpern, D.: Measurements of near-surface wind stress over an upwelling region near the Oregon coast, J. Phys. Oceanogr., 6, 108–112, 1976.

Halpern, D.: Offshore Ekman transport and Ekman pumping off Peru during the 1997–1998 El Niño, Geophys. Res. Lett., 29(5), 1075, doi:10.1029/2001GL014097, 2002.

Hayes, S. P., McPhaden, M. J. and Wallace, J. M.: The influence of sea surface temperature on surface wind in the eastern equatorial Pacific: weekly to monthly variability. J. Climate 2, 1500–1506. 1989.

Hong, S. Y. and Lim, J.O.: The WRF single–moment 6–class microphysics scheme (WSM6). J. Korean Meteor. Soc., 42, 129–151, 2006.

Hormazabal, S., Shaffer, G. and Leth, O.: Coastal transition zone off Chile, J. Geophys. Res., 109, C01021, doi:10.1029/2003JC001956, 2004.

Horvath, K., Koracin, D., Vellore, R., Jiang, J. and Belu, R.: Sub-kilometer dynamical downscaling of near-surface winds in complex terrain using WRF and MM5 mesoscale models, J. Geophys. Res., 117, D11111, doi:10.1029/2012JD017432, 2012.

Iacono, M. J., Delamere, J. S., Mlawer, E. J., Shephard, M. W., Clough, S. A. and Collins, W. D.: Radiative forcing by long–lived greenhouse gases: Calculations with the AER radiative transfer models. J. Geophys. Res., 113, D13103, 2008

Jacox, M. G. and Edwards, C. A.: Upwelling source depth in the presence of nearshore wind stress curl, J. Geophys. Res., 117, C05008, doi:10.1029/2011JC007856, 2012.

Luis Bravo 6-8-2016 23:11
Con formato: Fuente: (Predeterminado) Times New Roman, Inglés (americano)

Luis Bravo 6-8-2016 23:11
Con formato: Fuente: (Predeterminado) Times New Roman

Luis Bravo 6-8-2016 23:10
Con formato: Interlineado: sencillo

Luis Bravo 6-8-2016 23:11
Con formato: Fuente: Times New Roman

Luis Bravo 7-8-2016 0:04
Con formato: Dividir palabras

Luis Bravo 7-8-2016 0:04
Eliminado:

Luis Bravo 7-8-2016 0:04
Eliminado:

Luis Bravo 6-8-2016 23:11
Con formato: Fuente: Times New Roman

Janjic, Z. I.: Comments on ‘‘Development and evaluation of a convection scheme for use in climate models.’’ J. Atmos. Sci., 57, 3686–3686, 2000.

Jin, X., Dong, C., Kurian, J., McWilliams, J. C., Chelton, D. B. and Li. Z.: SST-Wind Interaction in Coastal Upwelling: Oceanic Simulation with Empirical Coupling, J. Phys. Oceanogr. 39:11, 2957-2970, 2009.

Kalnay, E., and Coauthors: The NCEP/NCAR 40-Year Re- analysis Project. Bull. Amer. Meteor. Soc., 77, 437–471, 1996.

Koračin, D., Dorman, C. E. and Dever, E. P.: Coastal Perturbations of Marine-Layer Winds, Wind Stress, and Wind Stress Curl along California and Baja California in June 1999, J. Phys. Oceanogr., 34(5), 1152–1173, doi:10.1175/1520-0485(2004)034<1152:CPOMWW>2.0.CO;2, 2004.

Lo, J. C.-F., Yang, Z.-L. and Pielke, R. A. Sr.: Assessment of three dynamical climate downscaling methods using the Weather Research and Forecasting (WRF) model. J. Geophys. Res., 113, D09112, doi:10.1029/2007jd009216, 2008.

Marchesiello, P. and Estrade, P.: Upwelling limitation by geostrophic onshore flow, J. Mar. Res., 68, 37–62, doi:10.1357/002224010793079004, 2010.

Marchesiello P., Lefevre, L., Vega, A., Couvelard, X. and Menkes, C.: Coastal upwelling, circulation and heat balance around New Caledonia’s barrier reef. Mar. Poll. Bull. 61, 432– 448, 2010.

Mellor, G. L.: Numerical simulation and analysis of the mean coastal circulation off California, Cont. Shelf Res., 6, 689 –713, 1986.

Moraga-Opazo, J., Valle-Levinson, A., Ramos, M. and Pizarro-Koch, M.: Upwelling-Triggered near-geostrophic recirculation in an equatorward facing embayment, Cont. Shelf Res., 31: 1991–1999, doi: 10.1016/j.csr.2011.10.002, 2011.

Muñoz, R. and Garreaud, R.: Dynamics of the low-level jet off the subtropical west coast of South America, Mon. Weather Rev., 133, 3661–3677, doi:10.1175/MWR3074.1, 2005.

Nelson, C.S.: Wind stress and wind-stress curl over the California Current, NOAA Tech. Rep., NMFS SSRF-714, U.S. Dept. of Commerce, 87 pp, 1977.

Paulson, C. A.: The mathematical representation of wind speed and temperature profiles in the unstable atmospheric surface layer. J. Appl. Meteor., 9, 857–861, 1970.

Perlin, N., Skyllingstad, E., Samelson, R. and Barbour, P.: Numerical simulation of air-sea coupling during coastal upwelling, J. Phys. Oceanogr., 37(8), 2081–2093, doi:10.1175/JPO3104.1, 2007.

Luis Bravo 6-8-2016 23:11
Con formato: Fuente: Times New Roman

Luis Bravo 6-8-2016 23:11
Con formato: Fuente: (Predeterminado) Times New Roman, Inglés (americano)

Luis Bravo 6-8-2016 23:11
Con formato: Fuente: 12 pt, Inglés (americano)

Luis Bravo 6-8-2016 23:10
Con formato: Control de líneas viudas y huérfanas, No dividir palabras, Adjust space between Latin and Asian text, Adjust space between Asian text and numbers

Luis Bravo 6-8-2016 23:11
Con formato: Inglés (americano)

Luis Bravo 6-8-2016 23:11
Con formato: Fuente: 12 pt, Inglés (americano)

Luis Bravo 6-8-2016 23:11
Con formato: Inglés (americano)

Luis Bravo 6-8-2016 23:11
Con formato: Fuente: 12 pt, Inglés (americano)

Luis Bravo 6-8-2016 23:11
Con formato: Inglés (americano)

Luis Bravo 6-8-2016 23:11
Con formato: Fuente: (Asian) Chino (RPC)

Luis Bravo 6-8-2016 23:11
Con formato: Inglés (americano)

Luis Bravo 7-8-2016 0:05
Eliminado:

Luis Bravo 6-8-2016 23:11
Con formato: Fuente: Times New Roman

Luis Bravo 6-8-2016 23:11
Con formato: Fuente: (Predeterminado) Times New Roman, Inglés (americano)

Luis Bravo 6-8-2016 23:11
Con formato: Fuente: Times New Roman

Luis Bravo 6-8-2016 23:11
Con formato: Fuente: Times New Roman

Perlin N., Skyllingstad E.D. and Samelson, R.M.: Coastal atmospheric circulation around an idealized cape during wind-driven upwelling studied from a coupled ocean-atmosphere model. Mon Weather Rev 139(3), 809–829, 2011.

Pickett, M. and Paduan, J.D.: Ekman transport and pumping in the California Current based on the U.S. Navy's high-resolution atmospheric model (COAMPS), J. Geophys. Res., 108, C10 3327, doi: 10.1029/2003JC001902, 2003.

Rahn D.A., Garreaud R. and Rutllant J.: The low-level atmospheric circulation near Tongoy Bay / point Lengua de Vaca (Chilean coast 30◦S), Mon. Wea. Rev., 139: 3628–3647, doi: 10.1175/MWR-D-11-00059.1, 2011.

Rahn, D. and Garreaud, R.: A synoptic climatology of the near-surface wind along the west coast of South America, Int. J. Climatol., 34 doi: 10.1002/joc.3724, 2013.

Renault, L., Dewitte, B., Falvey, M., Garreaud, R., Echevin, V. and Bonjean, F.: Impact of atmospheric coastal jet off central Chile on sea surface temperature from satellite observations (2000–2007), J. Geophys. Res., 114, C08006, doi:10.1029/2008JC005083, 2009.

Renault, L., Dewitte, B., Marchesiello, P., Illig, S., Echevin, V., Cambon, G., Ramos, M., Astudillo, O., Minnis, P., and Ayers, J. K.: Upwelling response to atmospheric coastal jets off central Chile: A modeling study of the October 2000 event, J. Geophys. Res., 117, C02030, doi:10.1029/2011JC007446, 2012.

Renault, L., Hall, H. and McWilliams. J.C.: Orographic shaping of US West Coast wind profiles during the upwelling season. Clim. Dyn., doi: 10.1007/s00382-015-2583-4, 2015

Rutllant, J. and Montecino,V.: Multiscale upwelling forcing cycles and biological response off north-central Chile. Revista Chilena de Historia Natural 75: 217-231, 2002.

Rutllant, J. A., Muñoz, R. C. and Garreaud, R. D.: Meteorological observations on the northern Chilean coast during VOCALS-REx. Atmos. Chem. Phys., 13, 3409–3422, doi:10.5194/acp-13-3409-2013, 2013.

Shaffer, G., Hormazabal, S., Pizarro, O., Djurfeldt, L. and Salinas, S.: Seasonal and interannual variability of currents and temperature over the slope off central Chile, J. Geophys. Res., 104, 29,951–29,961, doi:10.1029/1999JC900253, 1999.

Skamarock, W. C. and Klemp, J. B.: A time-split nonhydrostatic atmospheric model for weather research and forecasting applications, J. Comput. Phys., 227, 3465–3485, doi:10.1016/j.jcp.2007.01.037, 2008.

Small, R. J., deSzoeke, S.P., Xie, S.P., O'Neill, L., Seo, H., Song, Q., Cornillon, P., Spall, M. and Minobe, S.: Air-sea interaction over ocean fronts and eddies. Dyn. Atmos. Oceans, 45, 274–319, 2008.

Luis Bravo 7-8-2016 0:05
Eliminado:

Luis Bravo 6-8-2016 23:11
Con formato: Fuente: 12 pt, Inglés (americano)

Luis Bravo 6-8-2016 23:11
Con formato: Inglés (americano)

Luis Bravo 6-8-2016 23:11
Con formato: Fuente: 12 pt, Inglés (americano)

Luis Bravo 6-8-2016 23:10
Con formato: EspacioPosterior: 0 pto, Interlineado: sencillo

Luis Bravo 6-8-2016 23:11
Con formato: Inglés (americano)

Luis Bravo 6-8-2016 23:11
Con formato: Fuente: 12 pt, Inglés (americano)

Luis Bravo 6-8-2016 23:11
Con formato: Inglés (americano)

Luis Bravo 6-8-2016 23:11
Con formato: Fuente: 12 pt, Inglés (americano)

Luis Bravo 6-8-2016 23:11
Con formato: Inglés (americano)

Luis Bravo 6-8-2016 23:11
Con formato: Fuente: 12 pt, Inglés (americano)

Luis Bravo 6-8-2016 23:11
Con formato: Inglés (americano)

Luis Bravo 6-8-2016 23:11
Con formato: Fuente: 12 pt, Inglés (americano)

Luis Bravo 6-8-2016 23:11
Con formato: Fuente: (Predeterminado) Times New Roman, Inglés (americano)

Luis Bravo 6-8-2016 23:11
Con formato: Fuente: (Predeterminado) Times New Roman

Smith, R.L.: Upwelling, Oceanogr. Mar. Bio. Ann. Rev., 6, 11-46, 1968.

Stark, J. D., Donlon, C. J., Martin, M. J. and McCulloch, M. E.: OSTIA: An operational, high resolution, real time, global sea surface temperature analysis system. OCEANS 2007-Europe, IEEE, 1–4, 2007.

Strub, P. T., Montecino, V., Rutllant, J. and Salinas, S.: Coastal ocean circulation off western south America, in The Sea, vol. 11, The Global Coastal Ocean: Regional Studies and Syntheses, edited by A. R. Robinson and K. H. Brink, pp. 273– 314, John Wiley, New York, 1998.

Sverdrup, H. U.: Wind-driven currents in a baroclinic ocean, with application to the equatorial currents of the eastern Pacific. Proc. Natl. Acad. Sci. USA, 33, 318–326, 1947.

Tewari, M., Chen, F., Wang, W., Dudhia, J., LeMone, M. A., Mitchell, K., Gayno, M. Ek, G., Wegiel, J. and Cuenca, R. H.: Implementation and verification of the unified NOAH land surface model in the WRF model. 20th conference on weather analysis and forecasting/16th conference on numerical weather prediction, pp. 11–15, 2004

Thiel, M., Macaya, E. ., Acuña, E., Arntz, W. E., Bastias, H., Brokordt, K., Camus, P. A., Castilla, J. C., Castro, L. R., Cortés, M., Dumont, C. P., Escribano, R., Fenández, M., Gajardo, J. A., Gaymer, C. F., Gómez, I., González, A. E., González, H., Haye, P. A., Illanes, J. C., Iriarte, J. L., Lancellotti, D. A., Luna-Jorquera, G., Luxoro, C., Manriquez, P. H., Marín, V., Muñoz, P., Navarrete, S. A., Perez, E., Poulin, E., Sellanes, J., Sepúlveda, H. H., Stotz, W., Tala, F., Thomas, A., Vargas, C. A., Vasquez, J. A. and Vega, J. M. A.: the Humboldt Current System of Northern-Central Chile Oceanographic Processes , Ecological Interactions, edited by R. N. Gibson, R. J. A. Atkinson, and J. D. M. Gordon, Oceanogr. Mar. Biol. An Annu. Rev., 45(3), 195–344, doi:Book_Doi 10.1201/9781420050943, 2007.

Toniazzo, T., Sun, F., Mechoso, C. R. and Hall, A.: A regional modeling study of the diurnal cycle in the lower troposphere in the south-eastern tropical Pacific. Clim. Dyn., 41, 1899–1922, doi:10.1007/s00382-012-1598-3, 2013.

Vazquez-Cuervo, J., Dewitte, B., Chin, T. M., Amstrong, E., Purca, S. and Alburqueque, E.: An analysis of SST gradient off the Peruvian coast; The impact of going to higher resolution, Remote Sensing of Environment, 131, 76-84, 2013.

Venegas, S.A, Mysak, L.A. and Straub, D.N.: Atmosphere-Ocean Coupled Variability in the South Atlantic. Journal of Climate, 10, 2904-2920, 1997.

Webb, E. K.: Profile relationships: The log-linear range, and extension to strong stability. Quart. J. Roy. Meteor. Soc., 96, 67–90, 1970.

Luis Bravo 7-8-2016 0:05
Eliminado:

Luis Bravo 7-8-2016 0:06
Eliminado:

Luis Bravo 7-8-2016 0:02
Eliminado: ... [21]

Luis Bravo 7-8-2016 0:06
Eliminado:

Luis Bravo 6-8-2016 23:11
Con formato: Inglés (americano)

Luis Bravo 7-8-2016 0:06
Eliminado: .

Luis Bravo 6-8-2016 23:11
Con formato: Inglés (americano)

Luis Bravo 6-8-2016 23:11
Con formato: Fuente: Times New Roman

Luis Bravo 6-8-2016 23:11
Con formato: Fuente: (Predeterminado) Times New Roman, Inglés (americano)

Luis Bravo 6-8-2016 23:11
Con formato ... [22]

Luis Bravo 6-8-2016 23:11
Con formato ... [23]

Luis Bravo 6-8-2016 23:11
Con formato: Inglés (americano)

Luis Bravo 6-8-2016 23:11
Con formato ... [24]

Luis Bravo 6-8-2016 23:11
Con formato: Inglés (americano)

Luis Bravo 6-8-2016 23:11
Con formato ... [25]

Luis Bravo 6-8-2016 23:11
Con formato: Inglés (americano)

Luis Bravo 6-8-2016 23:11
Con formato ... [26]

Luis Bravo 6-8-2016 23:11
Con formato: Inglés (americano)

Luis Bravo 6-8-2016 23:11
Con formato ... [27]

Luis Bravo 6-8-2016 23:11
Con formato: Inglés (americano)

Luis Bravo 6-8-2016 23:11
Con formato ... [28]

Luis Bravo 7-8-2016 0:06
Eliminado:

Luis Bravo 6-8-2016 23:11
Con formato ... [29]

Wallace, J., Mitchell, T. and Deser, C.: The influence of sea-surface temperature on surface wind in the eastern equatorial Pacific: Seasonal and interannual variability. J. Climate, 2, 1492–1499, 1989.

Winant, C.D., Dorman, C.E., Friehe, C.A. and Beardsley, R.C.: The marine layer off Northern California: an example of supercritical channel flow. J. Atmos. Sci. 45, 3588–3605, 1988.

Wood, R., Mechoso, C. R., Bretherton, C. S., Weller, R. A., Huebert, B., Straneo, F., Albrecht, B. A., Coe, H., Allen, G., Vaughan, G., Daum, P., Fairall, C., Chand, D., Gallardo Klenner, L., Garreaud, R., Grados, C., Covert, D. S., Bates, T. S., Krejci, R., Russell, L. M., de Szoeke, S., Brewer, A., Yuter, S. E., Springston, S. R., Chaigneau, A., Toniazzo, T., Minnis, P., Palikonda, R., Abel, S. J., Brown, W. O. J., Williams, S., Fochesatto, J., Brioude, J. and Bower, K. N.: The VAMOS Ocean-Cloud-Atmosphere-Land Study Regional Experiment (VOCALS-REx): goals, platforms, and field operations. Atmos. Chem. Phys., 11, 627–654, doi:10.5194/acp-11-627-2011, 2011.

Xie, S.P.: Satellite observations of cool ocean-atmosphere interaction. Bull Amer. Meteor. Soc., 85:195-208, 2004.

Zhang, D. L., and Anthes, R.A.: A high–resolution model of the planetary boundary layer– sensitivity tests and comparisons with SESAME–79 data. J. Appl. Meteor. 21, 1594–1609, 1982. 1982,

Luis Bravo 6-8-2016 23:11
Con formato: Fuente: 12 pt, Inglés (americano)

Luis Bravo 6-8-2016 23:10
Con formato: EspacioPosterior: 0 pto, Interlineado: sencillo

Luis Bravo 6-8-2016 23:11
Con formato: Inglés (americano)

Luis Bravo 6-8-2016 23:11
Con formato: Fuente: 12 pt, Inglés (americano)

Luis Bravo 6-8-2016 23:11
Con formato: Inglés (americano)

Luis Bravo 6-8-2016 23:11
Con formato: Fuente: 12 pt, Inglés (americano)

Luis Bravo 6-8-2016 23:11
Con formato: Inglés (americano)

Luis Bravo 6-8-2016 23:11
Con formato: Fuente: 12 pt, Inglés (americano)

Luis Bravo 6-8-2016 23:11
Con formato: Inglés (americano)

Luis Bravo 6-8-2016 23:11
Con formato: Fuente: 12 pt, Inglés (americano)

Luis Bravo 6-8-2016 23:11
Con formato: Inglés (americano)

Luis Bravo 6-8-2016 23:11
Con formato: Fuente: 12 pt, Inglés (americano)

Luis Bravo 31-7-2016 9:01
Eliminado:

Luis Bravo 7-8-2016 0:06
Eliminado:

Luis Bravo 6-8-2016 23:11
Con formato: Fuente: Times New Roman

Luis Bravo 7-8-2016 0:07
Eliminado: ,

Table 1: Information of the physics options and main features used in the simulations.

Parameterization	References
Microphysics: WRF Single-Moment 6-class scheme. A scheme with ice, snow and graupel processes suitable for high-resolution simulations.	(Hong et al. 2006)
Longwave/Shortwave radiation: Rapid Radiative Transfer Model (RRTMG). An accurate scheme using look- up tables for efficiency, accounts for multiple bands, trace gases, and microphysics species. It includes the Monte Carlo Independent Column Approximation MCICA method of random cloud overlap.	(Iacono et al. 2008).
Boundary layer: University of Washington Turbulent kinetic energy (TKE) Boundary Layer scheme. This scheme is TKE based, and it is characterized by the use of moist-conserved variables, an explicit entrainment closure, downgradient diffusion of momentum, and con- served scalars within turbulent layers.	(Bretherton and Park 2009)
Surface layer: Based on Monin-Obukhov with Carslon-Boland viscous sub-layer and standard similarity functions from look-up tables.	(Paulson, C. A., 1970) (Dyer, A. J. et al., 1970) (Webb, E. K., 1970) (Beljaars, A.C.M., 1994) (Zhang and Anthes 1982)
Land surface model: The NOAH Land Surface Model. For land surface processes including vegetation, soil, snowpack and land atmosphere energy, momentum and moisture exchange.	(Tewari, M. et al., 2004)
Cumulus: Betts-Miller-Janjic scheme. Operational Eta scheme. Column moist adjustment scheme relaxing towards a well-mixed profile.	(Janjic, Z. I., 2000)

FIGURE CAPTIONS

Figure 1. Study area showing bathymetry and topography of the coastal terrain. The dotted thick line indicates the western boundary of the coastal band where satellite information (~25 km offshore) is absent. Red squares indicate the location of the three weather stations at Loma de Hueso, Punta Lengua de Vaca and Parral Viejo. The inset plot shows the three model domains used in the WRF simulations (36, 12 and 4 km).

Figure 2. Comparisons of the spatial patterns of the mean velocity fields of winds obtained (to same period 2007-2009) from a) QuikSCAT b) WRF simulation for the 36 km grid configuration. c) Root Mean Square (RMS) differences between observations and model results. The lower panels show dispersion plots between the observed and modeled N-S winds at d) Loma de Hueso, e) Parral Viejo and f) Punta Lengua de Vaca (Fig.1). Red line represent to linear regress and black line is 1:1 relation.

Figure 3. Mean wind stress curl obtained by the model (from 2007-2012) using three model domains a) 36 km, b) 12 km and c) 4 km. The yellow dotted line represents the length scale of the wind drop-off determined from a threshold value of -0.3 x 10^{-4} s^{-1} (Renault et al., 2015). d) Mean zonal profiles of alongshore wind speed obtained from the three model configurations (36, 12 and 4 km) and QuikSCAT observations are shown. e) Zonal profiles of alongshore wind speed from a weather station obtained onboard of a fishing boat during 22 April (black line), 18 May (black dashed line), 15 September (red line) and 28 October (red dashed line) of 2014 are also shown. The segmented line in d) and e) indicates the location of the satellite blind spot.

Figure 4. Wind stress annual cycle obtained from the simulation at 4 km resolution (from 2007-2012). Color represents the magnitude of wind stress (in Nm^{-2}) and the arrows indicate the wind stress direction.

Figure 5. Annual cycle of Ekman pumping (vertical velocity in md^{-1}) obtained from the simulation at 4 km resolution (from 2007-2012).

Luis Bravo 6-8-2016 22:45
Con formato: Fuente: 12 pt, Inglés (americano)

Luis Bravo 6-8-2016 22:45
Con formato: Fuente: 12 pt

Luis Bravo 6-8-2016 22:45
Con formato: Fuente: 12 pt, Inglés (americano)

Luis Bravo 6-8-2016 22:45
Con formato: Fuente: 12 pt

Luis Bravo 6-8-2016 22:45
Con formato: Fuente: 12 pt, Inglés (americano)

Luis Bravo 6-8-2016 22:45
Con formato: Fuente: 12 pt

Luis Bravo 7-8-2016 21:20
Eliminado: 09

Luis Bravo 6-8-2016 22:45
Con formato: Fuente: 12 pt

Luis Bravo 6-8-2016 22:45
Con formato: Fuente: 12 pt, Inglés (americano)

Luis Bravo 6-8-2016 22:45
Con formato: Fuente: 12 pt

Luis Bravo 7-8-2016 21:18
Eliminado: using daily average

Luis Bravo 7-8-2016 21:19
Eliminado: 7

Luis Bravo 6-8-2016 22:45
Con formato: Fuente: 12 pt

Luis Bravo 7-8-2016 21:19
Eliminado: 09

Luis Bravo 6-8-2016 22:45
Con formato: Fuente: 12 pt

Luis Bravo 6-8-2016 22:45
Con formato: Fuente: 12 pt, Inglés (americano)

Luis Bravo 6-8-2016 22:45
Con formato: Fuente: 12 pt

Luis Bravo 7-8-2016 21:19
Eliminado: using daily average

Luis Bravo 7-8-2016 21:19
Eliminado: 09

Luis Bravo 6-8-2016 22:45
Con formato: Fuente: 12 pt

Figure 6. Hovmoller diagrams of alongshore wind stress seasonal cycle (top panels) and the zonal gradient of alongshore wind (lower panels) for the regions at 28.5ºS (a, d), 30.5ºS (b, e) y 32.5ºS (c, f). The monthly mean zonal wind stress and mean zonal gradient are also shown (side black line).

Figure 7. Contributions of the Ekman transport and Ekman pumping to the vertical transport near the coast. a) Integrated orography index (H_{index}, black line) and coastaline meander index (M_{index}, red line, see text). b) Drop-off spatial length. c) Alongshore wind at Ld (red line) and coastal (black line). d) Ratio between Ekman pumping and Ekman transport e) Seasonal vertical transport associated with Ekman transport and f) seasonal vertical transport associated with Ekman pumping. To estimate the Ekman transport the wind stress closest to the coast was used, while Ekman pumping was integrated from the coast to the longitude corresponding to a distance from the coast equal to the length of the drop-off (see text).

Figure 8. Contributions of Ekman transport and Ekman pumping to the vertical transport near the coast (in Sv) over the study area (27.75°S-32.5°S, see Fig. 7). Seasonal vertical transport associated with Ekman transport (black line), Ekman pumping (red line) and total wind induced vertical transport (blue line, sum of both vertical transports). The estimates were carried out from the WRF simulation at 4 km resolution.

Figure 9. Annual cycle of sea surface temperature obtained using data from the Multi-scale Ultra-high Resolution (MUR). Top and bottom panels used a different colormap scale.

Figure 10. October mean spatial distribution for a) wind stress and b) Ekman pumping using the 4 km grid spacing simulation and c) sea surface temperature (SST) and d) SST gradient obtained from MUR observations.

Figure 11. First SVD mode between Ekman pumping (WEk) from the WRF simulation at 4 km resolution and sea surface temperature (SST) from MUR data. a) The Ekman

Luis Bravo 7-8-2016 0:07
Eliminado:

Luis Bravo 6-8-2016 22:45
Con formato: Fuente: 12 pt, Inglés (americano)

Luis Bravo 6-8-2016 22:45
Con formato: Fuente: 12 pt

Luis Bravo 6-8-2016 22:36
Eliminado: .

Luis Bravo 6-8-2016 22:45
Con formato: Fuente: 12 pt, Inglés (americano)

Luis Bravo 6-8-2016 22:45
Con formato: Fuente: 12 pt

Luis Bravo 6-8-2016 22:45
Con formato: Fuente: 12 pt, Inglés (americano)

Luis Bravo 6-8-2016 22:45
Con formato: Fuente: 12 pt

Luis Bravo 7-8-2016 0:10
Con formato: EspacioPosterior: 0 pto, Interlineado: 1,5 líneas

pumping spatial component. b) The SST spatial component. c) The black (red) line represents the associated Ekman pumping (SST) time series. Note that the units are arbitrary.

Luis Bravo 7-8-2016 0:10
Eliminado: ... [30]

Luis Bravo 6-8-2016 22:45
Con formato: Fuente: 12 pt

FIGURES

Figure 1.

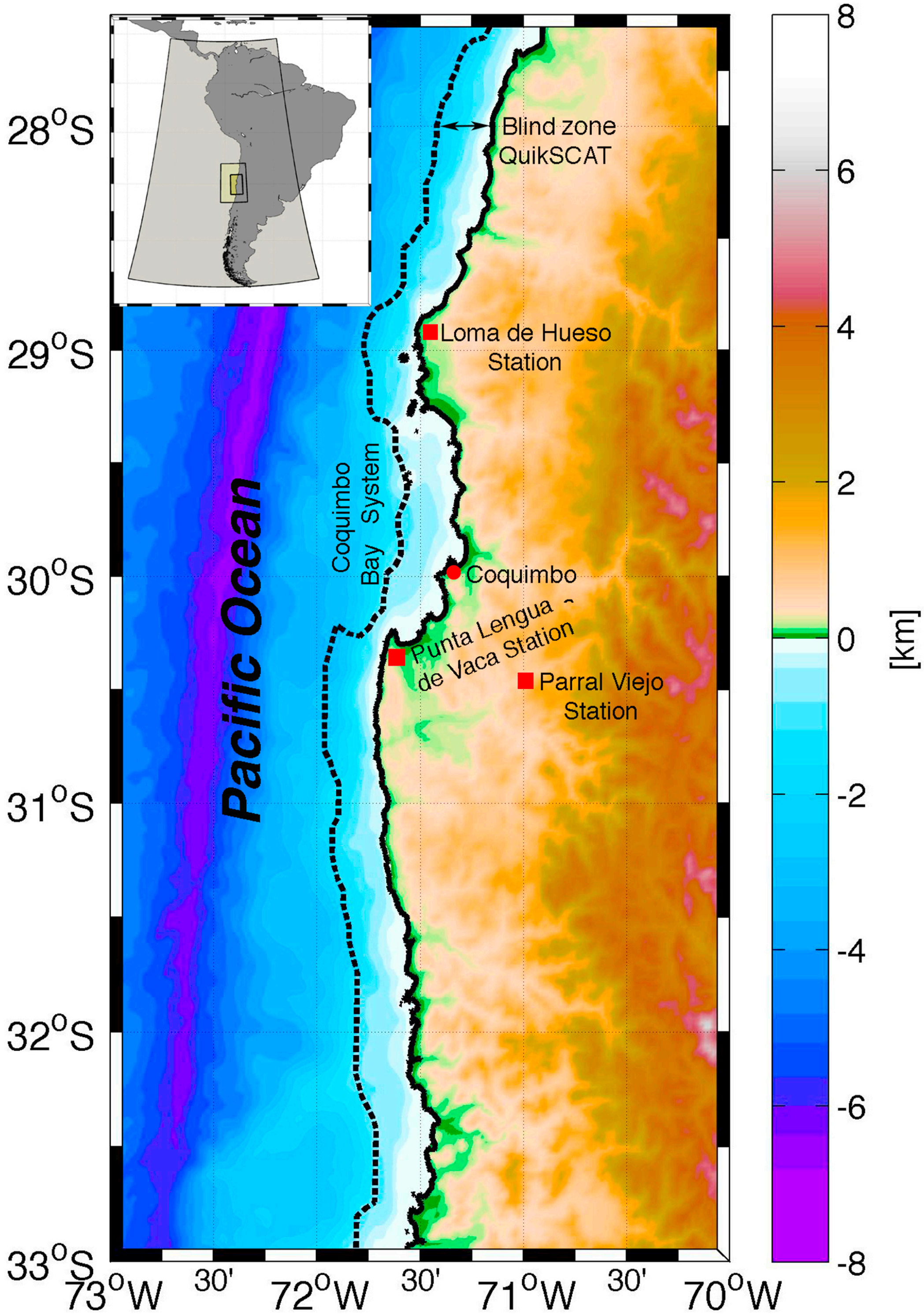

Figure 2.

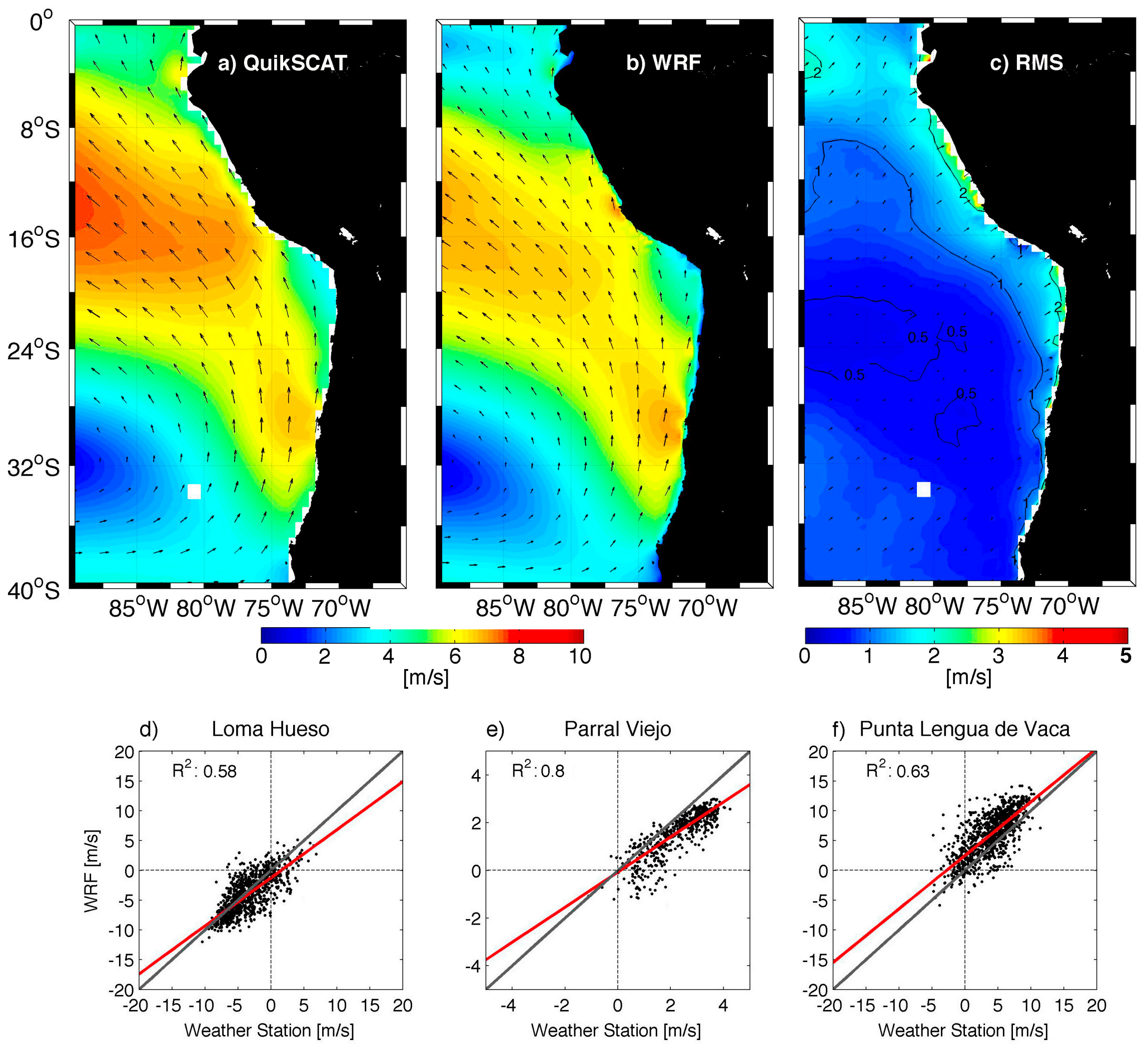

0°
8°S
16°S
24°S
32°S
40°S
a) QuikSCAT
b) WRF
c) RMS
85°W 80°W 75°W 70°W
85°W 80°W 75°W 70°W
85°W 80°W 75°W 70°W
0 2 4 6 8 10
[m/s]
0 1 2 3 4 5
[m/s]
d) Loma Hueso
e) Parral Viejo
f) Punta Lengua de Vaca
R²: 0.58
R²: 0.8
R²: 0.63
WRF [m/s]
Weather Station [m/s]
Weather Station [m/s]
Weather Station [m/s]

Figure 3.

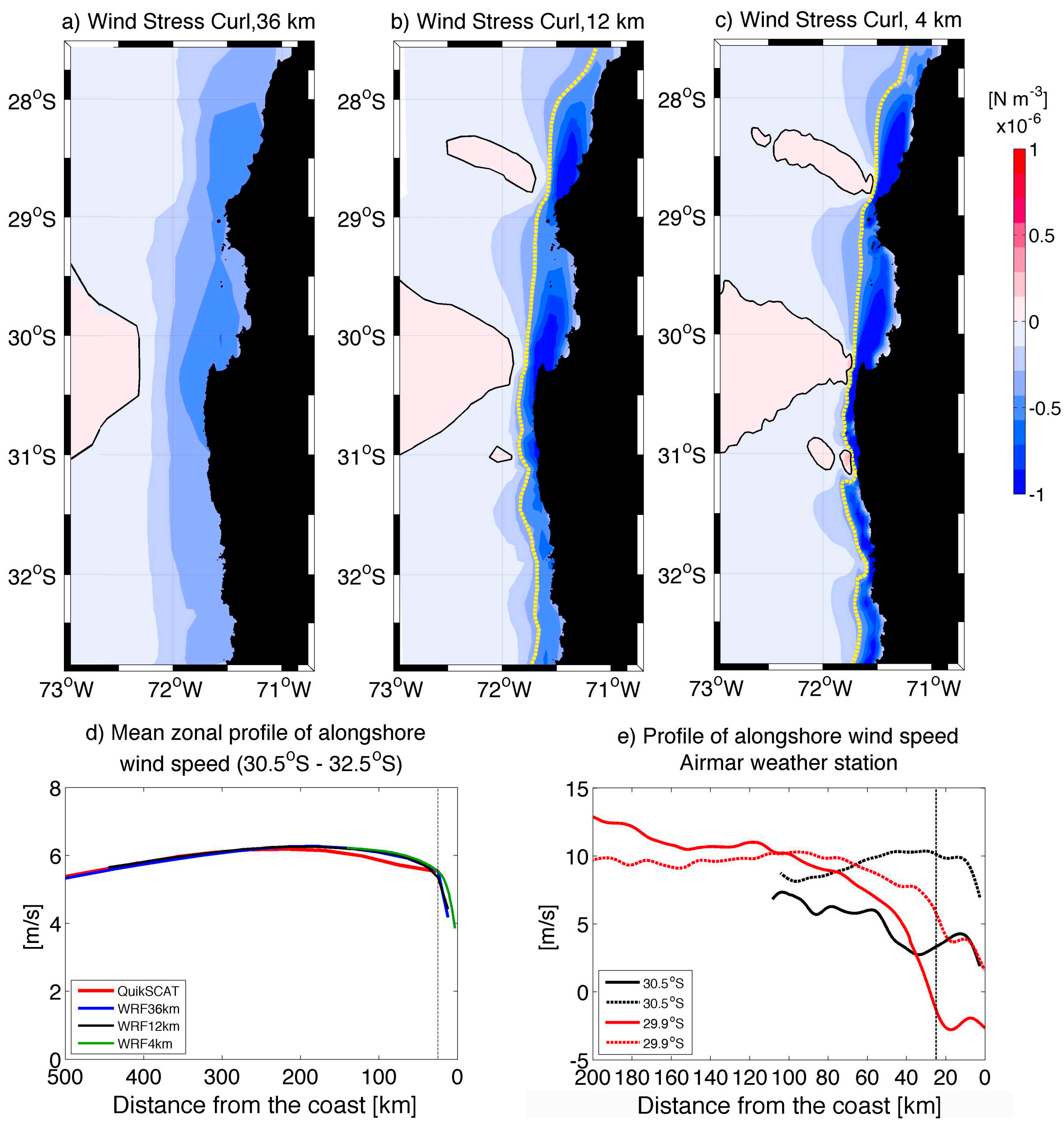

a) Wind Stress Curl,36 km
b) Wind Stress Curl,12 km
c) Wind Stress Curl, 4 km
28°S
29°S
30°S
31°S
32°S
73°W
72°W
71°W
[N m^{-3}]
x10^{-6}
1
0.5
0
-0.5
-1
d) Mean zonal profile of alongshore
wind speed (30.5°S - 32.5°S)
[m/s]
QuikSCAT
WRF36km
WRF12km
WRF4km
Distance from the coast [km]
e) Profile of alongshore wind speed
Airmar weather station
30.5°S
30.5°S
29.9°S
29.9°S
Distance from the coast [km]

Figure 4.

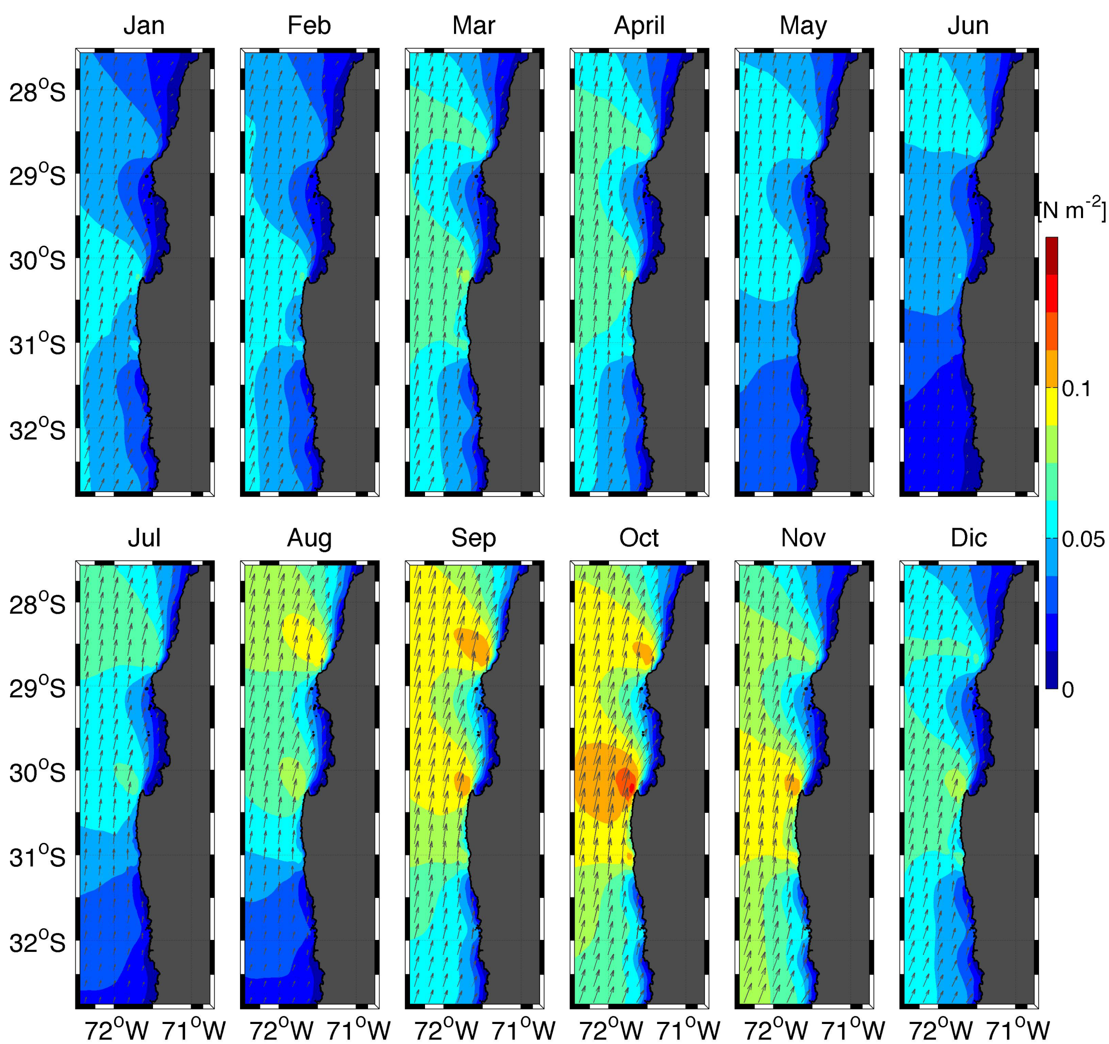

Jan
Feb
Mar
April
May
Jun
Jul
Aug
Sep
Oct
Nov
Dic
28°S
29°S
30°S
31°S
32°S
72°W
71°W
[N m^{-2}]
0.1
0.05
0

Figure 5.

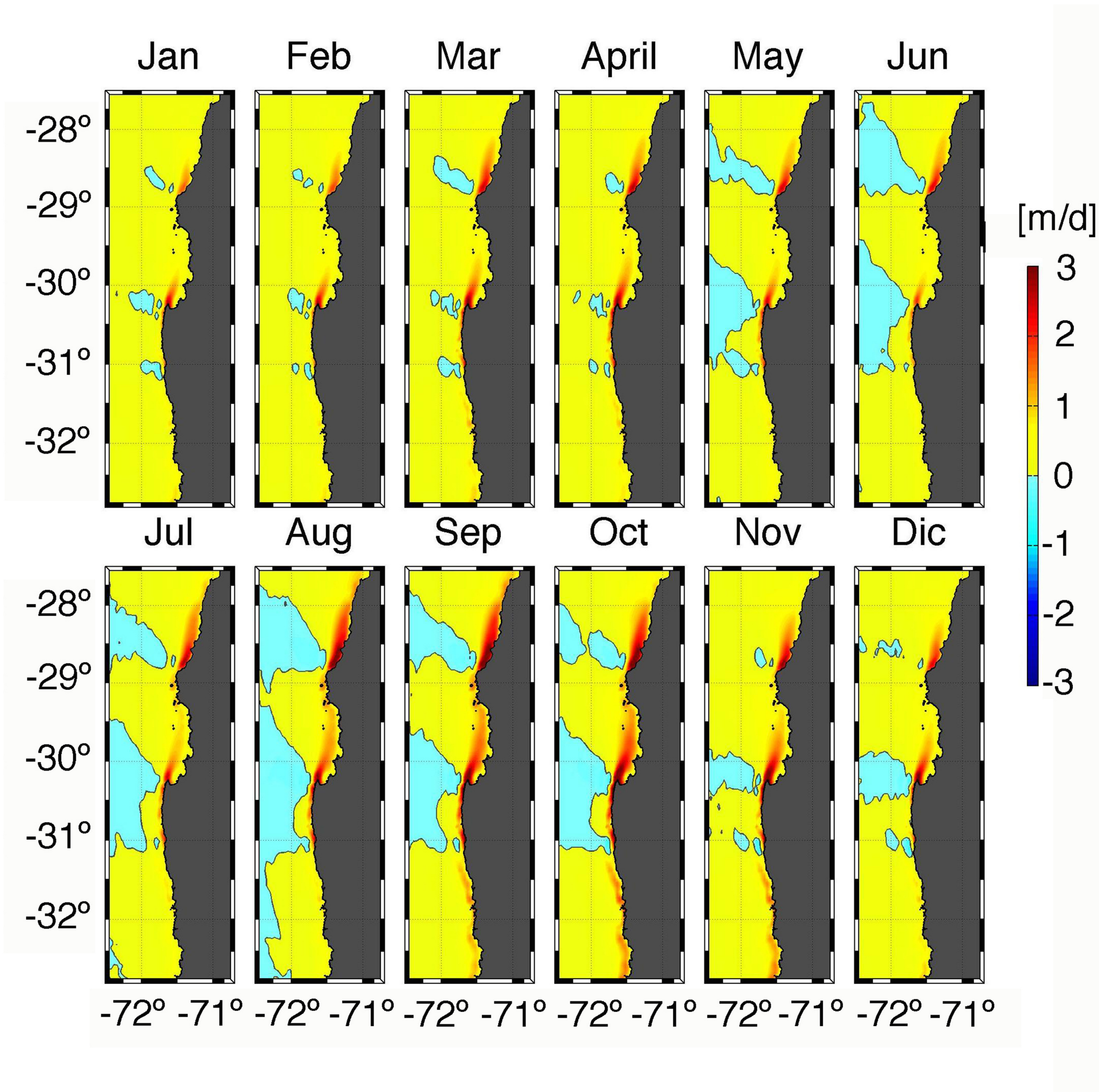

Jan
Feb
Mar
April
May
Jun
Jul
Aug
Sep
Oct
Nov
Dic
-28º
-29º
-30º
-31º
-32º
-72º -71º
[m/d]
3
2
1
0
-1
-2
-3

Figure 6.

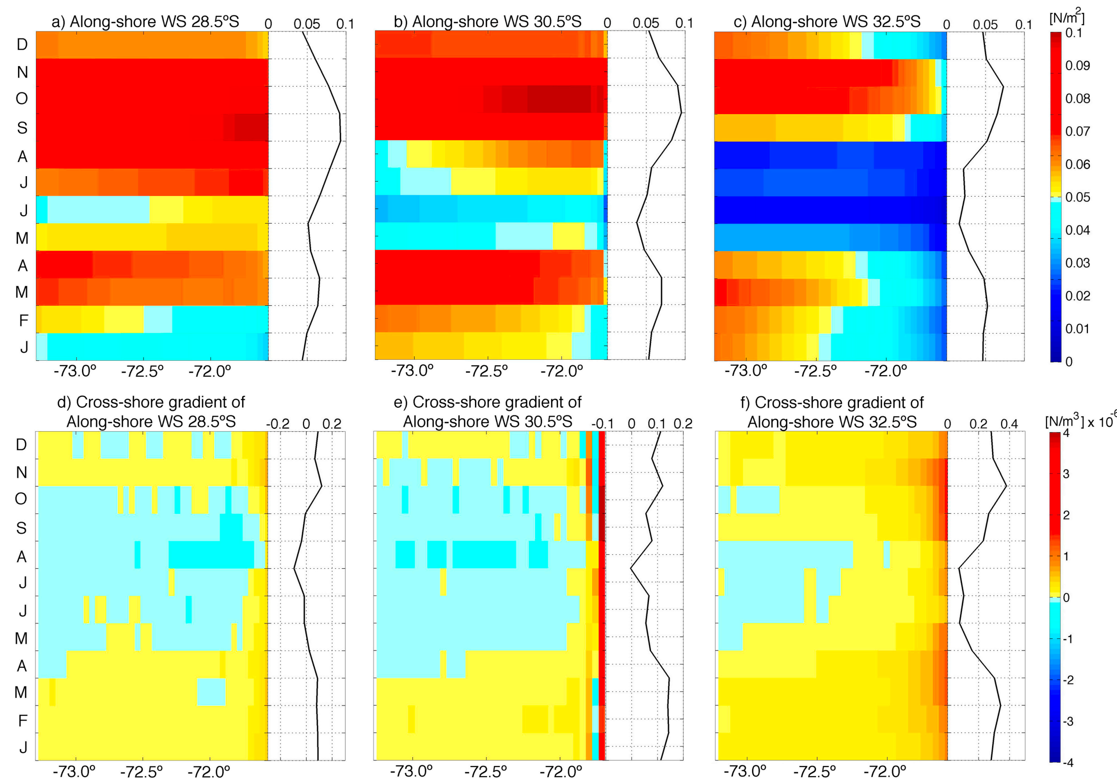

a) Along-shore WS 28.5ºS
b) Along-shore WS 30.5ºS
c) Along-shore WS 32.5ºS
d) Cross-shore gradient of Along-shore WS 28.5ºS
e) Cross-shore gradient of Along-shore WS 30.5ºS
f) Cross-shore gradient of Along-shore WS 32.5ºS
D N O S A J J M A M F J
-73.0º -72.5º -72.0º
0 0.05 0.1
-0.2 0 0.2
-0.1 0 0.1 0.2
0 0.2 0.4
[N/m2]
0.1 0.09 0.08 0.07 0.06 0.05 0.04 0.03 0.02 0.01 0
[N/m3] x 10-6
4 3 2 1 0 -1 -2 -3 -4

Figure 7.

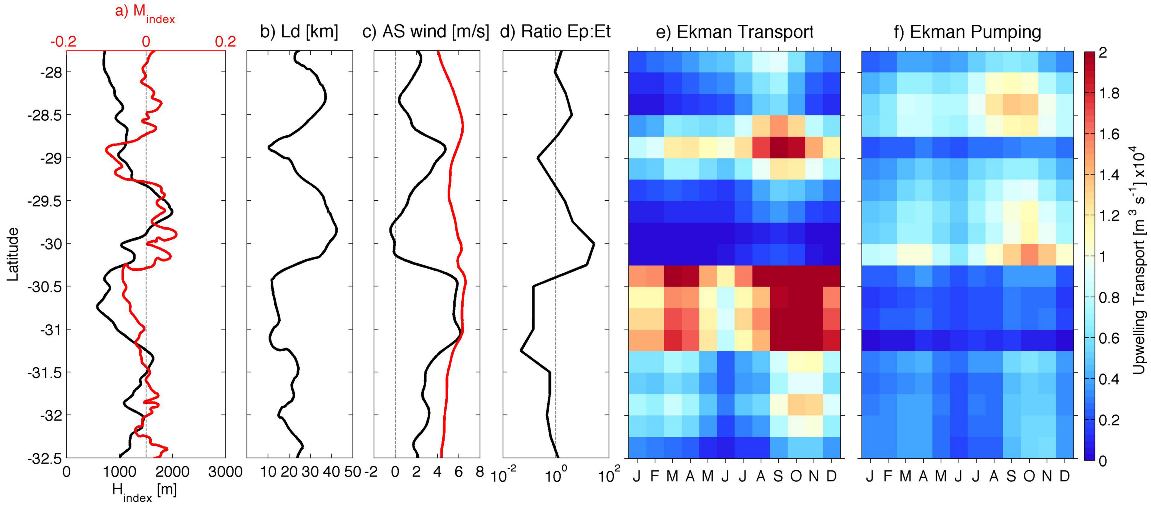

a) M$_{index}$
-0.2
0
0.2
b) Ld [km]
c) AS wind [m/s]
d) Ratio Ep:Et
e) Ekman Transport
f) Ekman Pumping
Latitude
-28
-28.5
-29
-29.5
-30
-30.5
-31
-31.5
-32
-32.5
0 1000 2000 3000
H$_{index}$ [m]
10 20 30 40 50
-2 0 2 4 6 8
10^{-2} 10^{0} 10^{2}
J F M A M J J A S O N D
J F M A M J J A S O N D
Upwelling Transport [m^3 s^{-1}] x10^4
2
1.8
1.6
1.4
1.2
1
0.8
0.6
0.4
0.2
0

Figure 8.

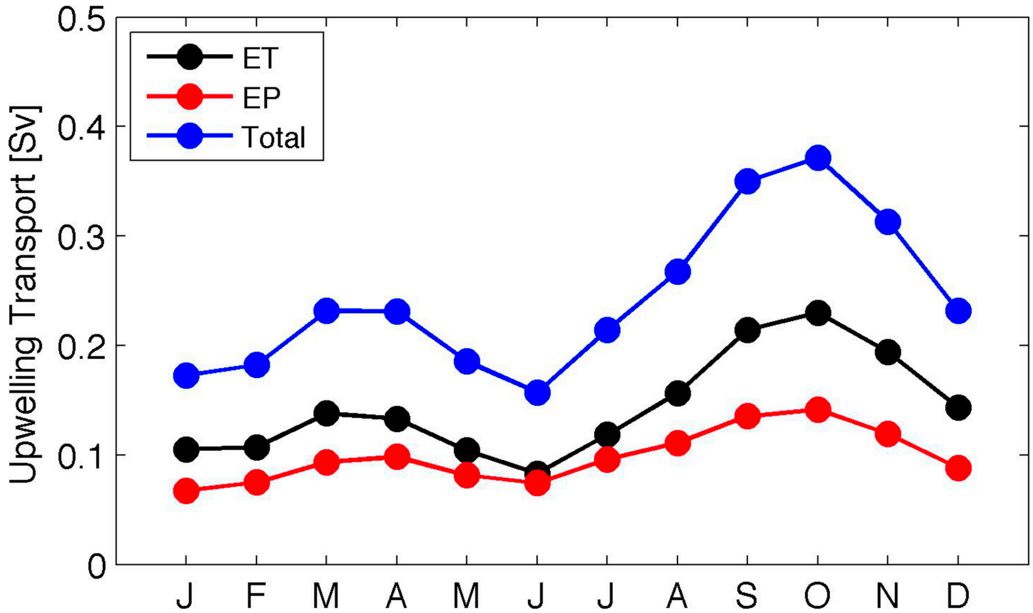

ET
EP
Total
Upwelling Transport [Sv]
0.5
0.4
0.3
0.2
0.1
0
J
F
M
A
M
J
J
A
S
O
N
D

Figure 9.

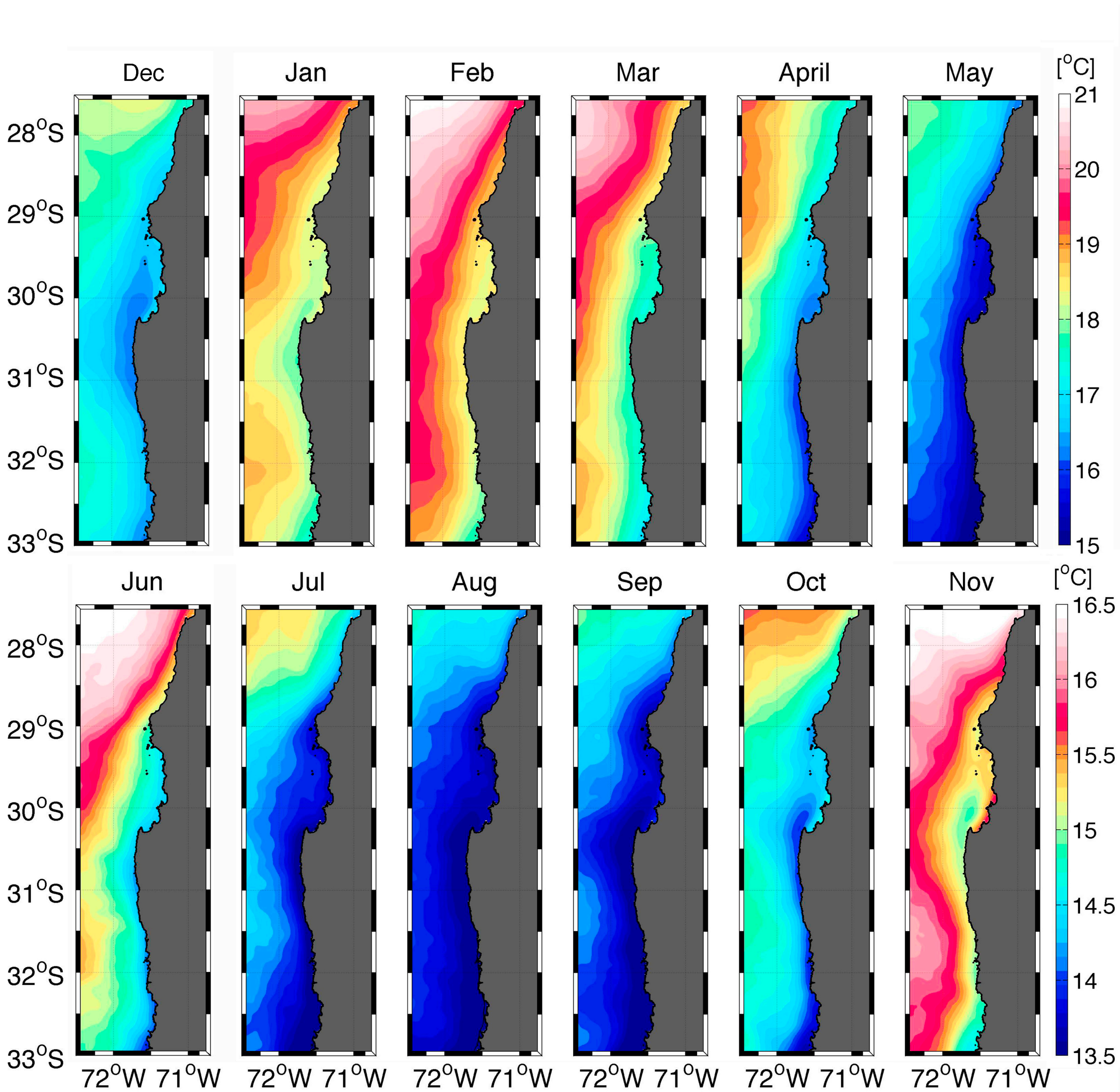

Dec
Jan
Feb
Mar
April
May
[°C]
21
20
19
18
17
16
15
28°S
29°S
30°S
31°S
32°S
33°S
Jun
Jul
Aug
Sep
Oct
Nov
[°C]
16.5
16
15.5
15
14.5
14
13.5
72°W 71°W

Figure 10.

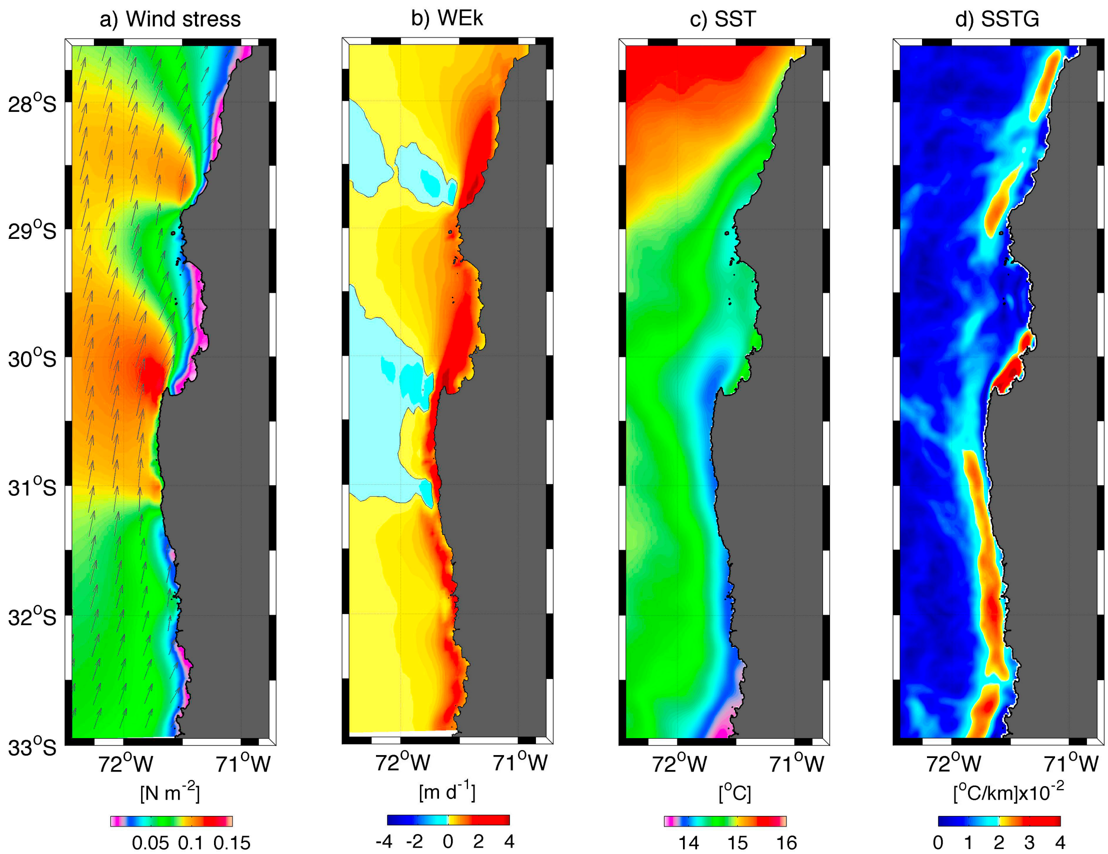

a) Wind stress
b) WEk
c) SST
d) SSTG
28°S
29°S
30°S
31°S
32°S
33°S
72°W
71°W
[N m-2]
0.05 0.1 0.15
[m d-1]
-4 -2 0 2 4
[°C]
14 15 16
[°C/km]x10-2
0 1 2 3 4

Figure 11.

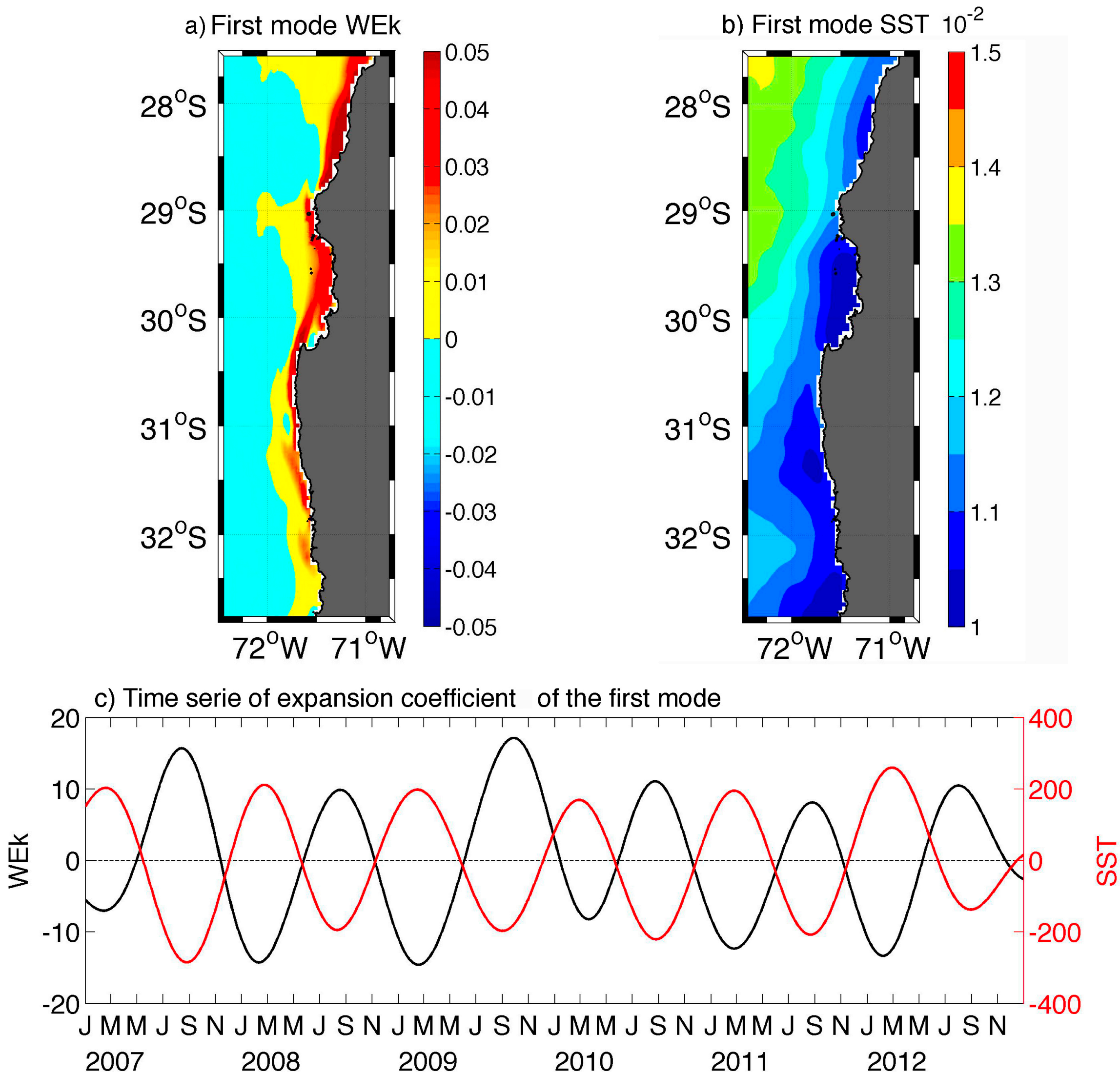

a) First mode WEk
28°S
29°S
30°S
31°S
32°S
72°W 71°W
0.05
0.04
0.03
0.02
0.01
0
-0.01
-0.02
-0.03
-0.04
-0.05
b) First mode SST
10^-2
1.5
1.4
1.3
1.2
1.1
1
c) Time serie of expansion coefficient of the first mode
WEk
SST
20
10
0
-10
-20
400
200
0
-200
-400
J M M J S N J M M J S N J M M J S N J M M J S N J M M J S N J M M J S N
2007 2008 2009 2010 2011 2012